

1 Global biogeography of N₂-fixing microbes: *nifH* amplicon database 2 and analytics workflow

3 Michael Morando^{1*}, Jonathan Magasin^{1*}, Shunyan Cheung^{1,2}, Matthew M. Mills³, Jonathan P. Zehr¹,
4 Kendra A. Turk-Kubo¹

5 ¹Ocean Sciences Department, University of California, Santa Cruz, Santa Cruz, 95064, United States

6 ²Institute of Marine Biology and Center of Excellence for the Oceans, National Taiwan Ocean University, Keelung, Taiwan

7 ³Earth System Science, Stanford University, Stanford, 94305, United States

8 * equal contributions

9 Correspondence to: Kendra A. Turk-Kubo (kturk@ucsc.edu)

10 **Abstract.** Marine ~~nitrogen~~ (N₂) fixation is a globally significant biogeochemical process carried out by a
11 specialized group of prokaryotes (diazotrophs), yet our understanding of their ecology is constantly evolving. Although
12 marine ~~dinitrogen~~ (N₂) N₂ fixation is often ascribed to cyanobacterial diazotrophs, indirect evidence suggests that
13 non-cyanobacterial diazotrophs (NCDs) might also be important. One widely used approach for understanding diazotroph
14 diversity and biogeography is polymerase chain reaction (PCR)-amplification of a portion of the *nifH* gene, which encodes a
15 structural component of the N₂-fixing enzyme complex, nitrogenase. An array of bioinformatic tools exists to process *nifH*
16 amplicon data, however, the lack of standardized practices has hindered cross-study comparisons. This has led to a missed
17 opportunity to more thoroughly assess diazotroph ~~biogeography, diversity~~ diversity, biogeography, and their potential
18 contributions to the marine N cycle. To address these knowledge gaps a bioinformatic workflow was designed that
19 standardizes the processing of *nifH* amplicon datasets originating from high-throughput sequencing (HTS). Multiple datasets
20 are efficiently and consistently processed with a specialized DADA2 pipeline to identify amplicon sequence variants
21 (ASVs). A series of customizable post-pipeline stages then detect and discard spurious *nifH* sequences and annotate the
22 subsequent quality-filtered *nifH* ASVs using multiple reference databases and classification approaches. This newly
23 developed workflow was used to reprocess nearly all publicly available *nifH* amplicon HTS datasets from marine studies,
24 and to generate a comprehensive *nifH* ASV database containing ~~7009~~ 9383 ASVs aggregated from 21 studies that represent
25 the diazotrophic populations in the global ocean. For each sample, the database includes physical and chemical metadata
26 obtained from the Simons Collaborative Marine Atlas Project (CMAP). Here we demonstrate the utility of this database for
27 revealing global biogeographical patterns of prominent diazotroph groups and highlight the influence of sea surface
28 temperature. The workflow and *nifH* ASV database provide a robust framework for studying marine N₂ fixation and
29 diazotrophic diversity captured by *nifH* amplicon HTS. Future datasets that target understudied ocean regions can be added
30 easily, and users can tune parameters and studies included for their specific focus. The workflow and database are available,

31 respectively, in GitHub (<https://github.com/jdmagasin/nifH-ASV-workflow>; Morando et al., 2024c) and Figshare
32 (<https://doi.org/10.6084/m9.figshare.23795943.v1.v2>; Morando et al., 2024a).

33 1 Introduction

34 Dinitrogen (N₂) fixation, the reduction of N₂ into bioavailable NH₃ is a source of new nitrogen (N) in the oceans and can
35 support as much as 70 % of new primary production in N-limited oligotrophic gyres (Jickells et al., 2017). Over millennia,
36 N₂ fixation may balance the loss of N from the marine system through denitrification and annamox (Zehr and Capone, 2020).
37 N₂ fixation was thought to be performed exclusively by prokaryotes, yet it was recently demonstrated that the marine
38 haptophyte alga, *Braarudosphaera bigelowii*, contains a cyanobacterially-derived organelle specialized for N₂ fixation
39 (Coale et al., 2024). Noting this exception, microorganisms able to fix N₂ (diazotrophs), are broadly characterized into two
40 main groups, cyanobacterial diazotrophs (those phylogenetically related to cyanobacteria) and non-cyanobacterial
41 diazotrophs (NCDs). Historically, cyanobacterial diazotrophs have been considered the most important contributors to
42 marine N₂ fixation (Villareal, 1994; Capone et al., 2005). NCDs, first detected by Zehr et al. (1998), have since been
43 demonstrated to be ubiquitous in pelagic marine waters, and are generally thought to be putative chemoheterotrophs with a
44 highly diverse lineage that includes the massive phylum Proteobacteria as well as Firmicutes, Actinobacteria, and
45 Chloroflexi (Turk-Kubo et al., 2022). However, their contribution of fixed N and their role in the global ocean is not
46 well-understood (Moisander et al., 2017).

47
48 Diazotrophs are often present at low abundances relative to other members of ocean microbiomes, which makes them
49 challenging to study (Moisander et al., 2017; Benavides et al., 2021). Distinctive pigments and morphologies that enable
50 some cyanobacterial diazotrophs to be identified by microscopy are lacking in many diazotrophs (Carpenter and Capone,
51 1983; Carpenter and Foster, 2002), including NCDs. Furthermore, many marine diazotrophs are uncultivated, which has
52 required the use of cultivation-independent approaches such as PCR and quantitative PCR (qPCR) (Luo et al., 2012; Shao
53 and Luo, 2022; Turk-Kubo et al., 2022). The *nifH* gene encodes the identical subunits of the Fe protein of nitrogenase, the
54 enzyme that catalyzes the N₂ fixation reaction, and contains both highly conserved and variable regions enabling its use as a
55 phylogenetic marker and as a proxy for N₂-fixing potential in marine ecosystems globally (Gaby and Buckley, 2011).

56
57 Although the importance of marine N₂ fixation is well-established, knowledge gaps remain, and discoveries continue to be
58 made (Zehr and Capone, 2020). For example, high-throughput sequencing (HTS) of *nifH* amplicons is expanding our
59 knowledge of diazotroph biogeography and activity and has revealed surprising new diversity. However, HTS studies often
60 utilize different or custom software pipelines and parameters, rendering direct comparisons between studies difficult.
61 Additionally, many studies do not address the full breadth of diazotrophic diversity because they focus on cyanobacterial
62 diazotrophs while providing only a superficial analysis of the NCDs present. The resulting lack of information on NCD *in*

63 *situ* distributions limits our understanding of diazotroph ecology and N₂ fixation as well as our ability to predict how these
64 populations will respond, e.g., trait-based ecological models, to a continually changing ocean.

65

66 To address these issues, we compiled published *nifH* amplicon HTS datasets along with two new datasets. Twenty-one
67 studies were reprocessed by our newly developed software workflow, which streamlines the integration of multiple, large
68 amplicon datasets for reproducible analyses. The workflow identifies amplicon sequence variants (ASVs) using a pipeline
69 developed around DADA2 (Callahan et al., 2016) — the DADA2 *nifH* pipeline — and then executes rigorous post-pipeline
70 stages to: remove spurious *nifH* ASVs; annotate the remaining quality-filtered ASVs using multiple reference databases and
71 classification approaches; and obtain *in situ* and modeled environmental data for each sample from the Simons Collaborative
72 Marine Atlas Project (CMAP; <https://simonscmap.com>). Although created to support research into N₂ fixation (*nifH*), the
73 complete workflow (ASV pipeline followed by the post-pipeline stages) can be adapted for use with other amplicon datasets,
74 including other functional genes or taxonomic markers (16S rRNA genes), with some simple modifications.

75

76 In addition to the workflow, our efforts resulted in the construction of a comprehensive database of *nifH* ASVs with
77 contextual metadata that will be a community resource for marine diazotroph investigations, enhancing comparability
78 between previous and future *nifH* amplicon datasets. The *nifH* ASV database is available in Figshare
79 (<https://doi.org/10.6084/m9.figshare.23795943.v1v2>; Morando et al., 2024a). The entire workflow required to produce the
80 *nifH* ASV database is available in two GitHub repositories, the DADA2 *nifH* pipeline
81 (https://github.com/jdmagasin/nifH_amplicons_DADA2; Morando et al., 2024b), and the post-pipeline stages
82 (<https://github.com/jdmagasin/nifH-ASV-workflow>; Morando et al., 2024c).

83 2 Data and Methods

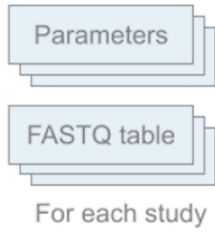
84 2.1 Overview of *nifH* amplicon workflow and *nifH* ASV database generation

85 The full workflow is comprised of two parts: 1) the DADA2 *nifH* pipeline; and 2) a series of post-pipeline stages (Fig. 1).

86

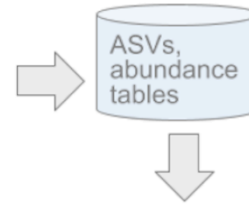
87

Configuration



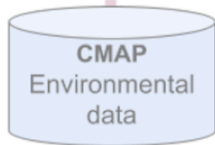
DADA2 *nifH* pipeline GitHub: [nifH_amplicons_DADA2](#)

1. Trim primers (cutadapt)
2. *Build sequencing error models: Reads → ORFs (FragGeneScan); Retain *nifH*-like reads (HMMER3)
3. FASTQ quality plots
4. Trim and filter reads
5. Dereplicate reads
6. Identify ASVs (denoising)
7. Merge forward / reverse ASVs
8. Make ASV abundance tables
9. Remove bimeras

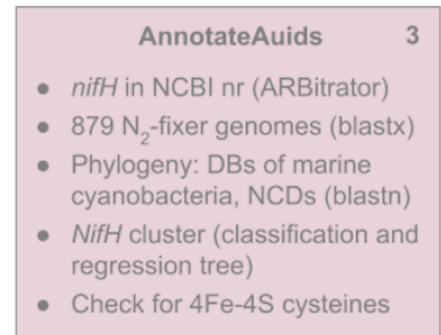
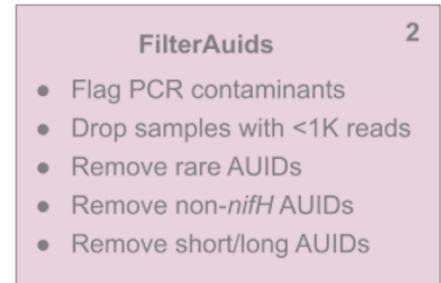
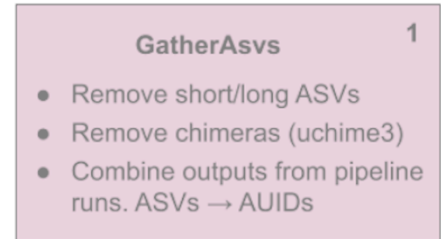
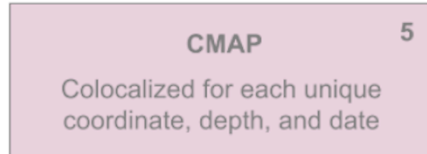


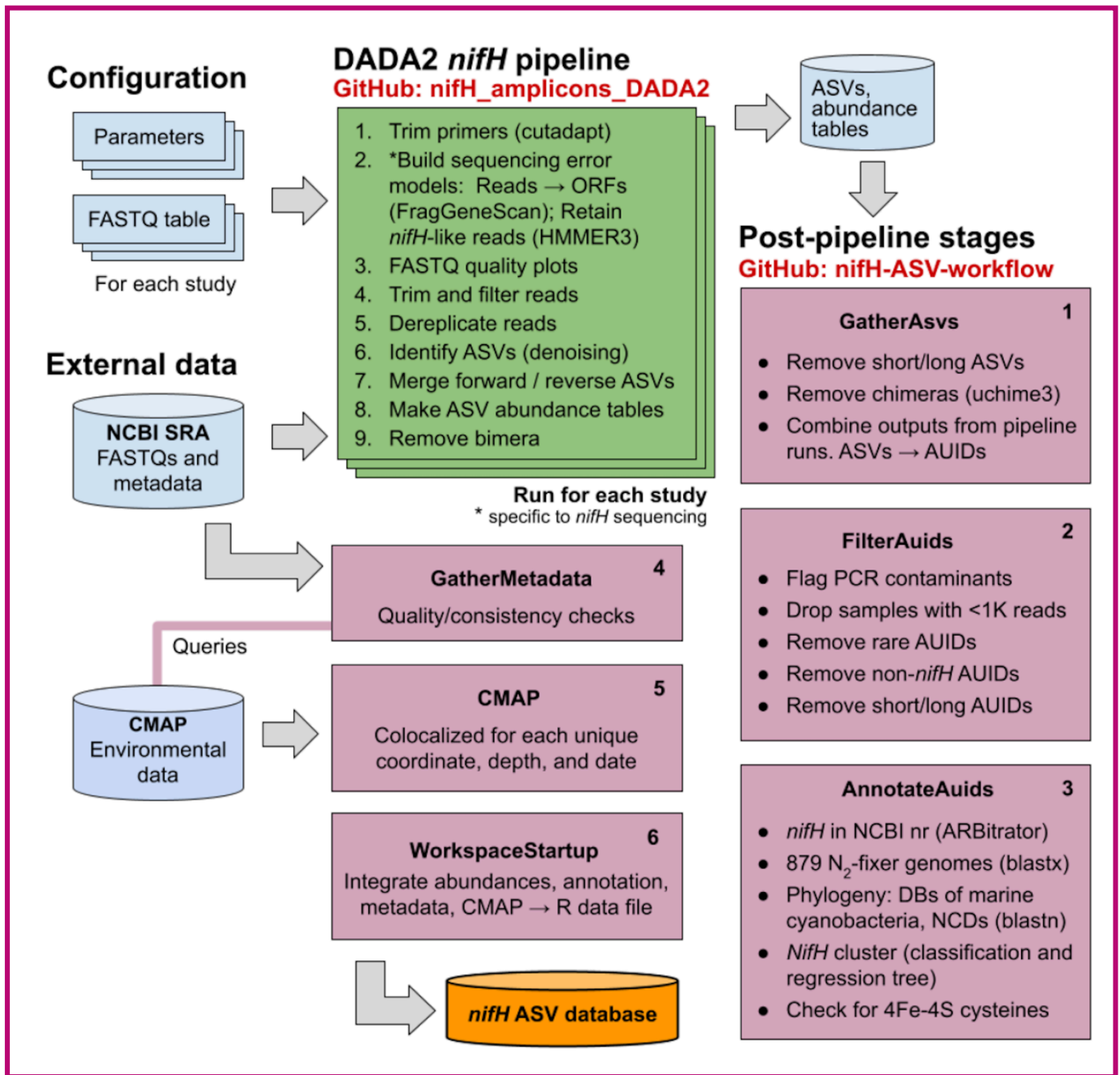
Post-pipeline stages GitHub: [nifH-ASV-workflow](#)

External data



Run for each study
* specific to sequencing





89

90 **Figure 1: Schematic of the *nifH* amplicon data workflow.** Data from all studies that met our criteria (Sect. 2.2) were downloaded from
 91 the NCBI Sequence Read Archive (SRA) and processed separately through the DADA2 *nifH* pipeline (green; Sect. 2.3.2), generally using
 92 identical parameters. ASV sequences and abundance tables from all studies were then combined and processed through each stage of the
 93 post-pipeline workflow (purple, Sect. 2.3.3) by executing the Makefile associated with each stage. Post-pipeline stages quality-filtered and
 94 then annotated the ASVs by reference to several *nifH* databases (DBs), and downloaded CMAP environmental data matched to the date,
 95 coordinates, and depth of each amplicon dataset. The main output of the entire workflow (pipeline and post-pipeline) is the *nifH* ASV
 96 database, which is available in Figshare (<https://doi.org/10.6084/m9.figshare.23795943.v1v2>; Morando et al., 2024a). The workflow is

97 maintained in two GitHub repositories, one for the DADA2 *nifH* pipeline (https://github.com/jdmagasin/nifH_amplicons_DADA2;
98 Morando et al., 2024b) and one for the post-pipeline stages (<https://github.com/jdmagasin/nifH-ASV-workflow>; Morando et al., 2024c).

99

100

101 Required inputs for the pipeline are raw *nifH* amplicon sequencing reads and sample collection metadata (at minimum the
102 latitude and longitude, depth and sample collection date and time) used to acquire environmental metadata from CMAP.
103 Criteria for including publicly available datasets are detailed in Section 2.2.1.

104

105 The DADA2 software package is frequently used for processing 16/18S rRNA gene amplicon sequencing data due to its
106 ability to remove base calling errors (“denoising”) and thereby infer error-free ASVs (Callahan et al., 2016). We have
107 developed a customizable pipeline to improve the error models utilized by DADA2 by training them only on reads in a
108 dataset that are valid *nifH* sequences (not PCR artifacts). The DADA2 pipeline runs from the command line in a Unix-like
109 shell, moving through nine steps (Fig. 1 DADA2 *nifH* pipeline) described in Section 2.3.2 for each study independently.
110 After the DADA2 pipeline is completed, outputs from all studies are integrated and refined by the six post-pipeline stages of
111 the workflow, which perform additional quality filtering (e.g., size- and abundance-based selection), identify and remove
112 spurious sequences (e.g., potential contaminants and non-target sequences), and annotate the ASVs (Fig. 1 Post-pipeline
113 stages). By considering ASVs from all studies simultaneously, the workflow considers rare ASVs that might be discarded as
114 irrelevant in a single-study analysis. Workflow stages are executed manually by running their associated Makefiles and
115 Snakefiles within a Unix-like shell.

116

117 The workflow generates the final data product published in this work, the *nifH* ASV database, which includes ASV
118 sequences, abundance and annotation tables, sample collection metadata, and sample environmental data from CMAP (Fig.
119 1). The database is available in Figshare (<https://doi.org/10.6084/m9.figshare.23795943.v1v2>; Morando et al., 2024a) as a set
120 of tables (comma-separated value files) and an ASV FASTA file. However, these are also provided within an R data file,
121 workspace.RData, in the WorkspaceStartup directory in the workflow GitHub repository, for users who wish to analyze,
122 curate, or customize the database using R packages for ecological analysis. All documentation, scripts, and data needed to
123 run the workflow and produce the *nifH* ASV database are provided in the workflow GitHub repository
124 (<https://github.com/jdmagasin/nifH-ASV-workflow>; Morando et al., 2024c). This includes pre-generated pipeline results for
125 each of the 21 studies as well as the pipeline parameters files.

126

127 In summary, the workflow facilitates the systematic and reproducible exploration of *nifH*-based diversity within microbial
128 communities and was applied to available *nifH* amplicon data to generate a globally distributed *nifH* ASV database. Together
129 the workflow and *nifH* ASV database will serve as valuable community resources, fostering future investigations while
130 ensuring comparability between previous and forthcoming studies. In the following sections, detailed descriptions of each
131 stage of the workflow are provided.

133 2.2 Compilation of *nifH* amplicon studies

134 2.2.1 Published studies

135 We compiled all publicly available *nifH* amplicon HTS data that were generated using the *nifH*1-4 primers (Zani, 1999; Zehr
 136 and ~~McReynolds~~McReynolds, 1989) and subsequently sequenced on the Illumina MiSeq/HiSeq platform totaling 1921
 137 studies (Table 1). Limiting the scope to investigations that used the same amplification primers enabled a more tractable
 138 comparison across studies by different research groups that employed varying approaches to sample collection and
 139 preparation for sequencing by different centers. Datasets were downloaded ~~directly~~ from the National Center for
 140 Biotechnology Information (NCBI) Sequencing Read Archive (SRA) using the GrabSeqs tool (Taylor et al., 2020) by
 141 specifying the study's NCBI project accession. Each dataset obtained included paired-end sequencing reads (in FASTQ files)
 142 and a table with the collection metadata for each sample. Some datasets could not be retrieved directly from the SRA and
 143 were obtained ~~directly~~ from the authors (Table A1). Note that we did not include studies where data was generated from
 144 experimental perturbations or particle enrichments (Table A1). Data were last accessed from NCBI SRA on 17 April 2024.

145

146 **Table 1: Information on the studies compiled to generate the *nifH* ASV database.** All compiled studies and associated information.
 147 This includes the study ID used to refer to each dataset, the number of samples, NCBI BioProject accession, a reference to each
 148 publication and its corresponding DOI.

149

Study ID	Samples	NCBI BioProject	Reference	DOI
AK2HI	43	PRJNA1062410	This study	n/a
BentzonTilia_2015	56	PRJNA239310	Bentzon-Tilia et al., 2015	10.1038/ismej.2014.119
Ding_2021	32	SUB7406573	Ding et al., 2021	10.3390/biology10060555
Gradoville_2020_G1	111	PRJNA530276	Gradoville et al., 2020	10.1002/lno.11423
Gradoville_2020_G2	56	PRJNA530276	Gradoville et al., 2020	10.1002/lno.11423
Hallstrom_2021	82	PRJNA656687	Hallstrøm et al., 2022b	10.1002/lno.11997
Hallstrom_2022	83	PRJNA756869	Hallstrøm et al., 2022a	10.1007/s10533-022-00940-w
Harding_2018	91	PRJNA476143	Harding et al., 2018	10.1073/pnas.1813658115
Mulholland_2018	29	PRJNA841982	Mulholland et al., 2019	10.1029/2018GB006130
NEMO	56	PRJNA1062391	This study	n/a
Raes_2020	121	PRJNA385736	Raes et al., 2020	10.3389/fmars.2020.00389
Sato_2021	28	PRJDB10819	Sato et al., 2021	10.1029/2020JC017071
Selden_2021	10	PRJNA683637	Selden et al., 2021	10.1002/lno.11727
Shiozaki_2017	22	PRJDB5199	Shiozaki et al., 2017	10.1002/2017GB005681
Shiozaki_2018GBC	20	PRJDB6603	Shiozaki et al., 2018b	10.1029/2017GB005869

Shiozaki_2018LNO	20	PRJDB5679	Shiozaki et al., 2018a	10.1002/Ino.10933
Shiozaki_2020	14	PRJDB9222	Shiozaki et al., 2020	10.1038/s41561-020-00651-7
Tang_2020	6	PRJNA554315	Tang et al., 2020	10.1038/s41396-020-0703-6
TianjUni_2016Turk Kubo_2021	14 136	PRJNA637983PRJ NA695866	Wu Turk-Kubo et al., 2021	10.1007/s10021-021-00702-z1 0.1038/s43705-021-00039-7
TianjUni_2017Wu_2 019	18	PRJNA438304	Wu et al., 2019	10.1007/s00248-019-01355-1
Turk_2021Wu_2021	136 14	PRJNA695866PRJ NA637983	Turk-Kubo Wu et al., 2021	10.1038/s43705-021-00039-71 0.1007/s10021-021-00702-z

150

151

152

153 Sample quality was validated prior to processing through the DADA2 *nifH* pipeline. Samples were discarded if they did not
154 contain unmerged pairs of forward and reverse reads with properly oriented primer sequences (Table A1). There were two
155 exceptions, studies by Shiozaki et al. (2017) and Shiozaki et al. (2018b), that used mixed-orientation sequence libraries and
156 required preprocessing. The reads in each of these studies were partitioned by whether they captured the coding or template
157 strand of *nifH*, determined by primer orientation. Because HTS sequence quality generally degrades from 5' to 3', the
158 partitioned data were run separately through the pipeline to preserve their sequencing error profiles for DADA2. The ASVs
159 from the misoriented reads (e.g. forward reads with template sequence) were then reverse-complemented and combined with
160 the properly oriented ASVs into a single ASV abundance table and FASTA file. Table 1 and Table A1 provide information
161 for obtaining the raw FASTQ files for all samples evaluated for the *nifH* ASV database including information regarding
162 studies excluded from the database.

163

164 2.2.2 Unpublished *nifH* amplicon datasets

165 Additional *nifH* gene HTS datasets were included from DNA samples collected on two cruises in the North Pacific. One was
166 a transect cruise across the Eastern North Pacific (NEMO; R/V New Horizon, August 2014; Shilova et al., 2017), and the
167 other was a transect cruise from Alaska to Hawaii (AK2HI; R/V Kilo Moana, September 2017). Euphotic zone samples were
168 collected from Niskin bottles deployed on a CTD-rosette (NEMO) or from the underway water system (5 m; AK2HI).
169 NEMO samples (2-4 L) were filtered through 0.2 µm and 3 µm pore-size filters (in series), while AK2HI samples (ca. 2 L)
170 were filtered through 0.2 µm pore-size filters using gentle peristaltic pumping. Filters were dried, flash frozen and stored at
171 -80°C until processing. DNA was extracted using a modified DNeasy Plant Kit (Qiagen, Germantown, MD) protocol,
172 described in detail in Moisander et al. (2008), with on-column washing steps automated by a QIACube (Qiagen).

173

174 Partial *nifH* DNA sequences were PCR-amplified using the *nifH*1-4 primers in a nested *nifH* PCR assay (Zani, 1999; Zehr
175 and ~~McReynolds~~McReynolds, 1989) according to details in Cabello et al. (2020). All samples were amplified in duplicate and

176 pooled prior to sequencing. A targeted amplicon sequencing approach was used to create barcoded libraries as described in
177 Green et al. (2015), using 5' common sequence linkers (Moonsamy et al., 2013) on second round primers, nifH1 and nifH2.
178 Sequence libraries were prepared at the DNA Service Facility at the University of Illinois at Chicago, and multiplexed
179 amplicons were bidirectionally sequenced (2×300 bp) using the Illumina MiSeq platform at the W.M. Keck Center for
180 Comparative and Functional Genomics at the University of Illinois at Urbana-Champaign. Samples were multiplexed to
181 achieve ca. 40,000 high quality paired reads per sample. The AK2HI and NEMO datasets can be found in the SRA
182 (BioProjects PRJNA1062410 and PRJNA1062391, respectively).

183

184 2.2.3 Sample collection data and co-localized CMAP environmental data

185 Sample collection data (e.g. coordinates, depth, date) and environmental data provide essential context for the interpretation
186 of diazotroph 'omics datasets. Large-scale multivariate analyses depend on properly formatted, complete, and ideally quality
187 checked metadata from consistently collected and analyzed measurements. However, accessibility to this information is often
188 limited (especially environmental data) for datasets published across multiple decades. Therefore, we first obtained sample
189 collection metadata from the SRA, and corrected or flagged errors and inconsistencies in the GatherMetadata stage of our
190 post-pipeline workflow (described below), to ensure consistency and completeness. For each sample, the geographic
191 coordinates, depth, and collection date (at local noon) from the SRA were used to query the Simons Collaborative Marine
192 Atlas Project on 24 March 2023 (CMAP; <https://simonscmap.com/>; Ashkezari et al., 2021) for co-localized environmental
193 data using a custom script (query_CMAP.py) in the CMAP stage of the workflow (Fig. 1). CMAP is an open-source data
194 portal designed for retrieving, visualizing, and analyzing diverse ocean datasets including research cruise-based and
195 autonomous measurements of biological, chemical, and physical properties, multi-decadal global satellite products, and
196 output from global-scale biogeochemical models. For each sample a mixture of 102100 satellite derived and modeled
197 environmental variables from the CMAP repository were obtained. These, along with the SRA collection data, are included
198 in our database. Aggregated metadata for all samples are summarized in Supplementary Table 1 but a detailed description of
199 environmental metadata can be found at the CMAP website (<https://simonscmap.com/catalog>). Metadata are available in the
200 *nifH* ASV database (metaTab.csv for sample metadata and cmapTab.csv for environmental data).

201

202 2.3 Automated workflow for processing datasets with the DADA2 *nifH* pipeline

203 2.3.1 Installation of the DADA2 *nifH* pipeline and the post-pipeline workflow

204 The workflow (Fig. 1) comprises two software projects installed from separate GitHub repositories,
205 *nifH_amplicons_DADA2* which ~~comprises~~contains the ASV pipeline and ancillary scripts, and *nifH-ASV-workflow* which
206 integrates pipeline results for all datasets with annotation and CMAP environmental data to produce the data deliverable of

207 the present work, the *nifH* ASV database. Installation requires cloning the `nifH_amplicons_DADA2` repository
 208 (https://github.com/jdmagasin/nifH_amplicons_DADA2; Morando et al., 2024b) to a local machine and then downloading
 209 several external software packages using `miniconda3`. Detailed installation instructions are available from the GitHub
 210 homepage, as well as a small tutorial to verify the installation on a small *nifH* amplicon dataset and introduce the two main
 211 pipeline commands (`organizeFastqs.R` and `run_DADA2_pipeline.sh`). Altogether the installation and example take 30–40
 212 min.

213
 214 After installing the ASV pipeline, installation of the *nifH*-ASV-workflow proceeds similarly: Clone the GitHub repository
 215 (<https://github.com/jdmagasin/nifH-ASV-workflow>; Morando et al., 2024c) and then download a few additional packages
 216 with `miniconda3` (~10 min to complete). For each study, the *nifH*-ASV-workflow includes the pipeline outputs (ASVs and
 217 abundance tables) which were used to create the *nifH* ASV database. Pipeline parameters and FASTQ input tables for each
 218 study are also provided for users who instead wish to rerun the pipeline starting from FASTQs downloaded from the SRA.
 219 Because the *nifH*-ASV-workflow includes data and parameters specific to the studies used in this work, it has a separate
 220 GitHub repository from the pipeline. However, we emphasize that together they comprise the *nifH* amplicon workflow in
 221 Fig. 1.

222
 223 Adding a new dataset to the workflow can be summarized in four steps: (1) Start a Unix-like shell that includes the required
 224 software (by “activating” a `miniconda3` environment called `nifH_ASV_workflow`). (2) Generate ASVs for the new dataset by
 225 running it through the pipeline, likely multiple times to tune parameters (Table 2). Output can be placed in the `Data` directory
 226 alongside other studies used in this work, and SRA metadata must be added to `Data/StudyMetadata`. (3) Include the new
 227 ASVs in the workflow by appending rows to the table `GatherASVs/asvs.noChimera.fasta_table.tsv`, which has file paths to
 228 all ASV abundance tables. (4) For each stage shown in Fig. 1, run the associated Makefile or Snakefile from the Unix-like
 229 shell by executing `"make"` or `"snakemake -c1 --use-conda"`, respectively. Documentation resides within each Makefile or
 230 Snakefile. Input tables from the post-pipeline workflow also have embedded documentation.

231
 232 **Table 2. Parameters for controlling the DADA2 *nifH* pipeline.** Default values can be overridden in the text file that is passed to
 233 `run_DADA2_pipeline.sh`. Parameters for “Read trimming” and “Error models” are used in steps 1 and 2 of the pipeline (Fig. 1). The
 234 remaining parameters are important for controlling how DADA2 trims and quality filters the reads, and merges forward and reverse
 235 sequences to create ASVs.

DADA2 <i>nifH</i> pipeline step	Parameter name	Default value	Description	Studies with non-default parameters
Read Trimming Remove primers with cutadapt	forward	TGYGAYCCN AARGCNGA	Forward primer 5' to 3'. Default is <i>nifH2</i> (Zehr and McReynolds, 1989).	None
	reverse	ADNGCCATC ATYTCNCC	Reverse primer 5' to 3'. Default is <i>nifH1</i> (Zehr and McReynolds, 1989).	None

	allowMissingPrimers	FALSE	If TRUE, retain read pairs even if primers are absent, e.g. if trimmed reads were uploaded to NCBI SRA.	Ding et al., 2021
Error Models	skipNifHErrorModels	FALSE	By default, use only <i>nifH</i> -like reads to train error models. If TRUE, use a random sample of all reads.	None
	NifH_minBits	150	Train error models using reads that align to PFAM00142 at \geq the specified bit score. The trusted cut off in PFAM00142 (25 bits) is always used to filter reads, then NifH_minBits. If set to 0, only the trusted cut off is used.	Set to 0 for most studies. Exceptions that used 100 bits were: Bentzon-Tilia et al., 2015; Gradoville et al., 2020; Shiozaki et al., 2018a; Turk-Kubo et al., 2021.
	NifH_minLen	33	Train error models using reads with ORFs that align with \geq this many residues to PFAM00142.	None
DADA2 filterAndTrim()	id.field	NA	Specify number of ID field if reads do not follow the CASAVA format. Forwarded to filterAndTrim(). If set, usually to 1.	Ding et al., 2021; Wu et al., 2021; Wu et al., 2019; Mulholland et al., 2019; Raes et al., 2020; Tang et al., 2020; Selden et al., 2021; Hallström et al., 2022b; Hallström et al., 2022a
	truncQ maxEE.fwd	2 Inf	Forwarded to filterAndTrim().	All studies set to 16 unless used truncLen 2.
	maxEE.fwd maxEE.rev	Inf		All studies set to 24 .
	maxEE.rev minLen	Inf 20	Forwarded to filterAndTrim().	All studies set to 4 .None
	minLen truncLen.fwd	200	Forwarded to filterAndTrim().	NoneAncillary script estimateTrimLengths.R determined optimal lengths.
	truncLen.fwd truncLen.rev	0		(See truncLen.fwd .)All studies used truncLen.
	truncLen.rev truncQ	0 2	Forwarded to filterAndTrim().	
useOnlyR1Reads	FALSE	If TRUE, only use R1 reads (and do not call mergePairs()). Used if R2 reads are very low quality.	None	
DADA2 mergePairs()	minOverlap	12	Forwarded to mergePairs().	None
	maxMismatch	0	Forwarded to mergePairs().	All studies set to 1.
	justConcatenate	FALSE	Forwarded to mergePairs().	None

236

237

238 2.3.2 DADA2 *nifH* pipeline

239 To encourage reproducible outputs and usage by non-programmers, the DADA2 pipeline (GitHub repository:
240 `nifH_amplicons_DADA2`) is controlled by a plain text parameters file (Table 2) and a descriptive table of input samples (the
241 “FASTQ map”). Since a study might include samples with vastly different diazotroph communities and relative abundances,
242 potentially impacting ASV inferences by DADA2, the FASTQ map for a study enables samples to be partitioned into
243 “processing groups” that are each run separately through DADA2. For example, in the present work processing groups

244 usually partitioned the samples in a study by the unique combinations of collection station or date, nucleic acid type (DNA or
245 RNA), size fraction, and collection depth. Pipeline outputs for each processing group are stored in a directory hierarchy with
246 levels that follow the processing group definition. Partitioning datasets into processing groups greatly improves the overall
247 speed of DADA2 and simplifies subsequent analyses that compare ASVs detected in different kinds of samples (e.g.,
248 detected versus transcriptionally active diazotrophs, or presence across different stations, depths, and/or size fractions). For
249 generating the *nifH* ASV database, studies that met selection criteria (Sect. 2.2.1 and Table 1) were run through the pipeline
250 using the study-specific FASTQ maps and parameters available in the Data directory of the *nifH*-ASV-workflow GitHub
251 repository.

252

253 The DADA2 pipeline runs from the command line in a Unix-like shell, moving through 9 main steps (Fig. 1 DADA2 *nifH*
254 pipeline): (1) trim reads of primers using cutadapt (Martin, 2011); (2) build sequencing error models; (3) make FASTQ
255 quality plots; (4) trim and filter reads based on quality; (5) dereplicate; (6) denoise (ASV inference); (7) merge forward and
256 reverse sequences; (8) make the ASV abundance table; and (9) remove chimera (Callahan et al., 2016 for steps 2 through 9).
257 These steps will be familiar to DADA2 users, except that for step 2 the error models are trained only on *nifH*-like reads
258 (discussed below). To run the pipeline on other functional genes, the parameters file would need to be edited to disable
259 *nifH*-based error models and to include the expected primers. We again note that the DADA2 pipeline is distinct from the
260 post-pipeline workflow stages which are specific to this work, but together they comprise the workflow in Fig. 1.

261

262 DADA2 parameters impact the ASV sequences identified, and the number of reads used. Thus, exploring parameters is
263 essential for checking the robustness of ASVs (particularly rare ones) and their relative abundances. The ~~DADA2 pipeline~~
264 ~~supports the optimization of parameters (Table 2). For example, one~~ method and parameters used to trim the reads are
265 especially important because most pipeline steps occur after filterAndTrim (Fig. 1). Two methods are supported: One can
266 trim each read based on its quality degradation (truncQ parameter to the DADA2 filterAndTrim function; Table 2) or all
267 reads at the same position determined by inspecting sample FASTQ quality plots: (truncLen parameter; Table 2, and
268 comparison of methods in Appendix B). The latter approach can be labor-intensive and unsystematic for studies with tens to
269 hundreds of samples. To address this the ancillary script estimateTrimLengths.R can be used to determine trimming lengths
270 that will maximize the percentage of reads that make it through the pipeline. For each FASTQ file in a study, the script
271 chooses 1 K read pairs at random and removes the primers. Then the read pairs are trimmed using every combination of
272 lengths over a window (from 55—85 % of the median read length in 15 bp steps) and successful merges (with ≥ 12 bp
273 overlapping and ≤ 2 mismatches) are counted. The counts are averaged across all samples (weighting by sequencing depths)
274 and the top ten combinations of forward and reverse trimming lengths are reported in a table, with estimates for the
275 percentages of reads retained and the mean errors per read to help choose the maxEE parameters (Table 2).

276

277 The pipeline allows one to rerun DADA2 steps 3–9, with outputs saved in separate, date-stamped directories. ~~Read~~
278 ~~trimming~~Primer removal and error models (steps 1–2) are unlikely to benefit much from parameter tuning, so the pipeline
279 reuses outputs from those steps. Log files and diagnostic plots created by the pipeline are intended to facilitate parameter
280 evaluation as well to capture statistics to support publication. Moreover, logs and other pipeline outputs are consistently
281 formatted across pipeline runs, which enables scripts to aggregate and analyze results across datasets such as in our
282 workflow.

283

284 Step 1 consisted only of ~~read-trimming~~primer removal using cutadapt (Martin, 2011). Raw reads were ~~trimmed and retained~~
285 ~~only when read pairs for which~~retained only if the forward (nifH2) and reverse (nifH1) primers were both found on the R1
286 and R2 reads, respectively. DADA2 sequencing error models were built at step 2 using only the reads predicted to be *nifH*,
287 rather than a subsample of all reads as in typical use of DADA2. Reads likely to encode *nifH* were identified as follows:
288 FragGeneScan (version 1.31, (Rho et al., 2010)) was used to predict open reading frames (ORFs) on R1 reads which were
289 then aligned to the nitrogenase PFAM model (PF00142.20) using HMMer3 (hmmsearch version 3.3.2; hmmer.org). ORFs
290 with >33 residues and a bit score that exceeded the trusted cut-off encoded in the model (25.0 bits) were retained.
291 Prefiltering the reads aims to reduce effects of PCR artifacts on the error models. For some studies this approach resulted in
292 increases (~3–10 %) in the total percentage of reads retained in ASVs, and fewer total ASVs, compared to using error
293 models based on a subsample of all reads. Adapting the pipeline to a different marker gene would only require substituting
294 an appropriate PFAM model, or disabling step 2 (by setting skipNifHErrorModels to TRUE; Table 2), which forces the
295 pipeline to make error models by subsampling from all reads. At step 4, DADA2 filterAndTrim() ~~truncated reads at the first~~
296 ~~base with PHRED score ≤16 and~~trimmed forward and reverse reads using the lengths suggested by estimateTrimLengths.R
297 and then discarded read pairs that had excessive errors (>2 for R1 reads, >4 for R2 reads) or were <20 bp. ~~The PHRED~~
298 ~~quality cut off, which corresponds to a 2.5 % base call error rate, was complemented by conservative~~
299 ~~parameters~~Conservative parameters were used for merging sequences: At most 1 base pair was allowed to mismatch in the
300 forward and reverse sequence overlap of minimally 12 bp (stage 7). Dereplicating (step 5) and denoising, ASV calling (step
301 6), generating an abundance table (step 8), and bimera detection (step 9), were all performed with default DADA2
302 parameters. ~~Data sets~~Datasets that passed pre-processing steps (Table 1) were run through the DADA2 pipeline using mostly
303 identical parameters (~~except for the trimming lengths (truncLen.fwd and truncLen.rev in Table 2).~~

304

305 2.3.3 Post-pipeline stages

306 The workflow post-pipeline stages (GitHub repository: nifH-ASV-workflow) combine the pipeline outputs, conduct further
307 quality control steps, co-locate the samples with environmental data from the CMAP data portal, and annotate the ASVs
308 (Fig. 1 Post-pipeline stages). Key outputs from the post-pipeline are: a unified FASTA with all the unique ASVs detected

309 across all the studies (i.e. all samples); tables of ASV total counts and relative abundances in all studies; multiple annotations
310 for each ASV by comparison to several *nifH* reference databases; and CMAP environmental data for each sample. These
311 outputs comprise the *nifH* ASV database, and are all available within an R image file (workspace.RData) generated by the
312 workflow which is included in the *nifH*-ASV-workflow repository. Provision as an R image will make the outputs
313 immediately accessible to many researchers who prefer R due to its extensive packages for ecological analysis. The *nifH*
314 ASV database is also available on Figshare (<https://doi.org/10.6084/m9.figshare.23795943.v1.v2>; Morando et al., 2024a).
315 The remainder of this section describes each of the post-pipeline stages.

316
317 The GatherAsvs stage aggregated ASV sequences and abundances across all DADA2 pipeline runs (i.e. from all samples and
318 studies). First, ASVs were filtered based on length. Chimera sequences were then removed using UCHIME3 denovo (Edgar,
319 20162016a) via VSEARCH (Rognes et al., 2016). Chimera sequences were identified within each sample, but the final
320 classification was based on majority vote (chimera or not) across the samples in the processing group. Second, the
321 GatherAsvs stage combined the non-chimeric ASVs from all studies into a single abundance table and FASTA file. Since
322 each study is run independently through the DADA2 pipeline, ASV identifiers are not consistent across studies. Therefore,
323 each unique ASV sequence was renamed with a new unique identifier of the form AUID.i, where AUID stands for **ASV**
324 **U**niversal **I**dentifier. The scripts used to rename the ASVs (assignAUIDs2ASVs.R) and to create the new abundance table
325 (makeAUIDCountTable.R) are available at the *nifH*_amplicons_DADA2 GitHub repository (in
326 scripts.ancillary/ASVs_to_AUIDs). The script assignAUIDs2ASVs.R optionally takes an AUID reference FASTA so that
327 AUIDs can be preserved as new datasets are added to future versions of the *nifH* ASV database.

328
329 Both rare and potential non-*nifH* sequences were assessed on the unified AUID tables in the next stage, FilterAuids (Fig. 1).
330 First, possible contaminants were identified by the Makefile invocation of check_nifH_contaminants.sh, provided as an
331 ancillary script in the pipeline GitHub repository. In brief, check_nifH_contaminants.sh first translated all ASVs into amino
332 acid sequences using FragGeneScan (Rho et al., 2010), which were then compared using *blastp* to 26 contaminants known
333 from previous *nifH* amplicon studies (Zehr et al., 2003; Goto et al., 2005; Farnelid et al., 2009; Turk et al., 2011). ASVs that
334 aligned at >96 % amino acid identity to known contaminants were flagged. Next FilterAuids removed samples with
335 ~~≤1000~~500 reads, and rare ASVs, defined as those that did not have at least one read in at least two samples or ≥1000 reads in
336 one sample.

337
338 Next, the ancillary script, classifyNifH.sh, was employed to identify and remove non-*nifH*-like sequences. The script utilized
339 *blastx* to search each ASV against ~44 K positive and ~15 K negative examples of NifH protein sequences that were found
340 in NCBI GenBank by ARBitrator (run on April 28, 2020; Heller et al., 2014). ASVs were classified based on the relative
341 quality of their best hits in the two databases, similar to the "superiority" check in ARBitrator. An ASV was classified as
342 positive if the E-value of its best positive hit was ≥10 times smaller than the E-value for the best negative hit, and vice versa
343 for negative classifications. ASVs failing to meet these criteria were classified as 'uncertain'. The *blastx* searches used the

344 same effective sizes for the two databases (-dbsize 1000000), so that E-values could be compared, and retained up to 10 hits
345 (-max_target_seqs 10).

346

347 The FilterAuids stage of the workflow exclusively discarded ASVs with negative classifications. “Uncertain” ASVs were
348 retained as potential *nifH* sequences not in GenBank. In the last stage, FilterAuids excluded ASVs with lengths that fell
349 outside 281–359 nucleotides, a size range which in our experience encompasses the majority of valid *nifH* amplicon
350 sequences generated by nested PCR with nifH1–4 primers.

351

352 For each AUID in the *nifH* ASV database, we provide taxonomical annotations using several different approaches,
353 encompassed by the AnnotateAuids stage (Fig. 1) and accessible through ancillary scripts in the GitHub repository (in
354 scripts.ancillary/Annotation). The script blastxGenome879.sh enables a protein level comparison via *blastx* against a
355 database of 879 sequenced diazotroph genomes (“genome879”, <https://www.jzehrlab.com/nifHnifH>). Here, the closest
356 cultivated relative for each AUID was determined by smallest E-value among alignments with ≥ 50 % amino acid identity
357 and ≥ 90 % query sequence coverage. Cautious interpretation is suggested because the reference ~~DB-database~~ is small and
358 contains only cultivable taxa. Similarly, the top nucleotide match of each AUID was identified by E-value within alignments
359 possessing ≥ 70 % nt identity and ≥ 90 % query sequence coverage obtained by *blastn* against a curated database of *nifH*
360 sequences (July 2017 *nifH* database, https://www.zehr.pmc.ucsc.edu/nifH_Database_Public/www.jzehrlab.com/nifH) by
361 executing the blastnARB2017.sh script. Additionally, *nifH* cluster annotations were assigned to each ASV using the
362 classification and regression tree (CART) method of Frank et al. (2016). This approach was implemented as part of a custom
363 tool that predicted ORFs for the ASVs with FragGeneScan, then performed a multiple sequence alignment on the ORFs, and
364 then applied the CART classifier. The tool is available as the ancillary script assignNifHclustersToNuclSeqs.sh.

365

366 The Makefile created and searched against two "phylotype" databases, one containing 223 *nifH* sequences from prominent
367 marine diazotrophs including NCDs (Turk-Kubo et al., 2022) and another with 44 UCYN-A *nifH* oligotype sequences
368 (Turk-Kubo et al., 2017). These databases were searched using *blastn* with the effective database size of the ARB2017
369 database (-dbsize set to ~29 million bases) to enable E-value comparisons across all three searches. For each ASV, we
370 provide phylotype annotations based on the top hit by E-value if the alignment had ≥ 97 % nt identity and covered ≥ 70 % of
371 the ASV. Finally, ORFs for all ASVs were searched for highly conserved residues which are thought to coordinate the
372 4Fe-4S cluster in NifH, specifically for paired cysteines shortly followed by AMP residues (described in Schlessman et al.
373 1998). This simple check, performed by the script check_CCAMP.R, was intended to complement the reference-based
374 annotations above. Presence of cysteines and AMP could be used to retain ASVs that have no close reference. Absence could
375 be used to flag ASVs that, despite high similarity to a reference sequence, might not represent functional *nifH* (e.g. due to
376 frameshifts).

377

378 Since the annotation scripts provided multiple taxonomic identifications for most of the AUIDs, a primary taxonomic ID was
379 assigned for each AUID using the script `make_primary_taxon_id.py`. If a phylotype annotation (e.g., Gamma A) was
380 assigned, this became the primary taxonomic ID; otherwise, cultivated diazotrophs from genome879 were used (e.g.,
381 “*Pseudomonas stutzeri*”). Finally, when neither a phylotype nor a cultivated diazotroph could be determined, the *nifH* cluster
382 (e.g. “unknown 1G”) was used. AUIDs without an assigned *nifH* cluster or taxonomic rank below domain were removed
383 from the final *nifH* ASV database unless paired cysteines and AMP were detected. This final data filtration step occurred in
384 the WorkspaceStartup stage described below.

385
386 The CMAP stage was managed by a Snakefile that called the script `query_cmap.py` to query the CMAP data portal for
387 co-localized environmental data (Fig. 1). The script was passed the main output from the GatherMetadata stage,
388 `metadata.cmap.tsv`, a table of the collection coordinates, dates at local noon, and depths from all the samples.
389 GatherMetadata reported any samples with missing metadata and ensured standardized formats for the required query fields.
390 Additionally, `query_cmap.py` validated fields prior to querying CMAP. It should be noted that the precision of values
391 obtained from CMAP depend on floating point arithmetic, not the significant digits of the underlying measurement or model.
392 Therefore, prior to an analysis requiring high precision for specific CMAP variables, it is recommended to consult the
393 original producer of the data to determine the significant digits.

394
395 The last stage of the workflow, WorkspaceStartup, filtered out AUIDs that had no annotation and then generated the final
396 *nifH* ASV database, which is comprised of AUID abundance tables (counts and relative), AUID annotations, sample
397 metadata and corresponding environmental data. These data are provided as text files (.csv and FASTA) within a single
398 compressed file (.tgz) that is available in Figshare (<https://doi.org/10.6084/m9.figshare.23795943.v1v2>; Morando et al.,
399 2024a) as well as within the workflow GitHub repository within an R image file (`workspace.RData`).

400 2.4 Diazotroph biogeography from DNA dataset of the *nifH* ASV database

401 The DNA dataset, a custom version of the *nifH* ASV database restricted to DNA samples (representing a majority of the
402 database, only removing 94108 cDNA samples out of 944 total samples), was created to showcase the utility of the
403 workflow. Additional data reduction steps were conducted, averaging replicates and samples from the same location but
404 different size fractions, to enable comparisons between different sampling methodologies.

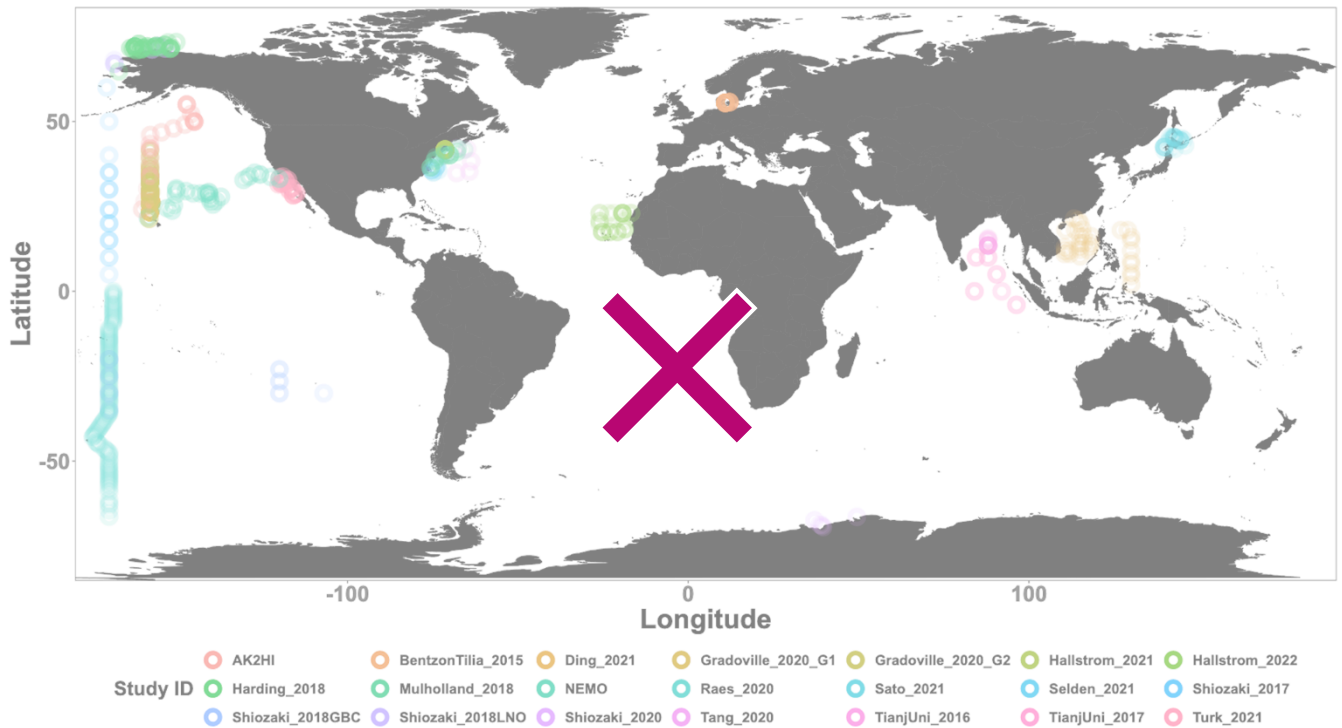
405 3 Results and Discussion

406 3.1 Generation of the marine *nifH* ASV database

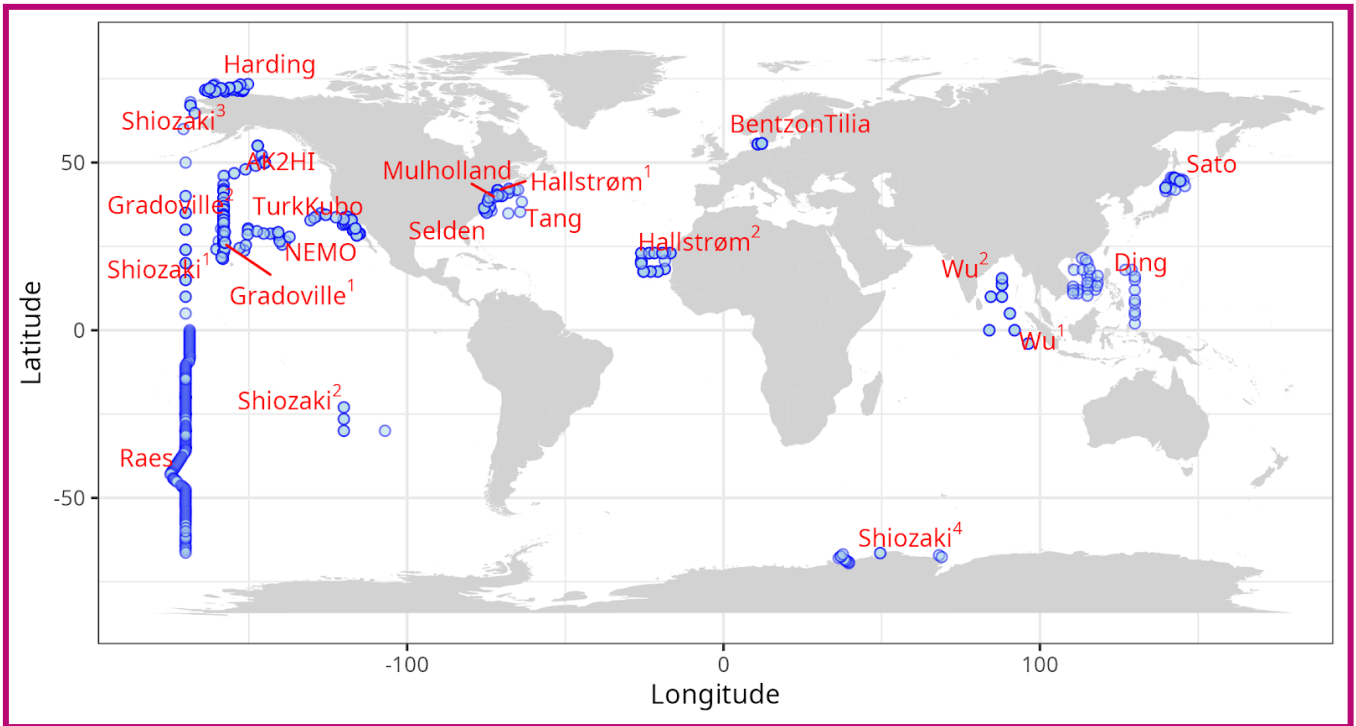
407 All publicly available marine *nifH* amplicon HTS data from studies that met our criteria, including two new studies, were
408 compiled in the present investigation (see Sect. 2.2 and Table A1). Altogether 982 samples from 21 studies, comprising a

409 total of 87.7 million reads (Table 3), were processed through the entire workflow, i.e., the DADA2 *nifH* pipeline (Sect. 2.2.2)
410 as well as the post-pipeline stages (Sect. 2.2.3). The *nifH* ASV database, i.e., the ASV sequences, abundances, and
411 annotations, as well as sample collection and CMAP environmental data, was generated from the 865944 samples, 79099383
412 ASVs, and 34.443.0 million reads that were retained by this workflow (Figs. 1 and 2 and Table 3). To our knowledge it is the
413 only global database for marine diazotrophs detected using *nifH* HTS amplicon sequencing, with comprehensive,
414 standardized ancillary data (Fig. 2 and Supplementary Table 1).

415



416



417

418 **Figure 2: Global sampling distribution of the *nifH* ASV database.** World map of sampling locations for the datasets compiled and
 419 processed to construct the *nifH* ASV database. Abbreviated study IDs are used with superscripts ordered by publication year for Shiozaki

420 (2017, 2018GBC, 2018LNO, and 2020), Hallström (2021 and 2022), and Wu (2019 and 2021). For Gradoville the superscripts indicate
 421 Gradients cruises 1 and 2. See Table 1 for the citation source linked to each study ID.

422

423

424 **Table 3: Summary of the full *nifH* workflow.** The number of samples, ASVs, and reads retained through the entire workflow (the
 425 DADA2 *nifH* pipeline and major post-pipeline stages) to create the *nifH* ASV database. The vast majority ASVs that were removed by
 426 GatherAsvs fell outside 200–450 nt. WorkspaceStartup removed ASVs with no annotation and samples that had zero reads after ASV
 427 filtering.

	Initial	DADA2 pipeline	Gather Asvs	FilterAuids				Workspace Startup
				<1K<500 reads in sample	rare	non-NifH	length	
Samples	982	982	982	89 4951	890 951	890 951	890 951 1	86 5944
ASVs	n/a	177,935 1 52,915	97,205 1 39,355	97,172 139, 334	13,774 1 8,193	12,479 16, 253	9,416 1 1,915	7,909 9,383
Reads (millions)	87.7	43.3 48.7	38.7 48. 4	38.6 48.4	36.4 45.5	36.0 45.0	35.1 43 .8	34.4 43.0

428

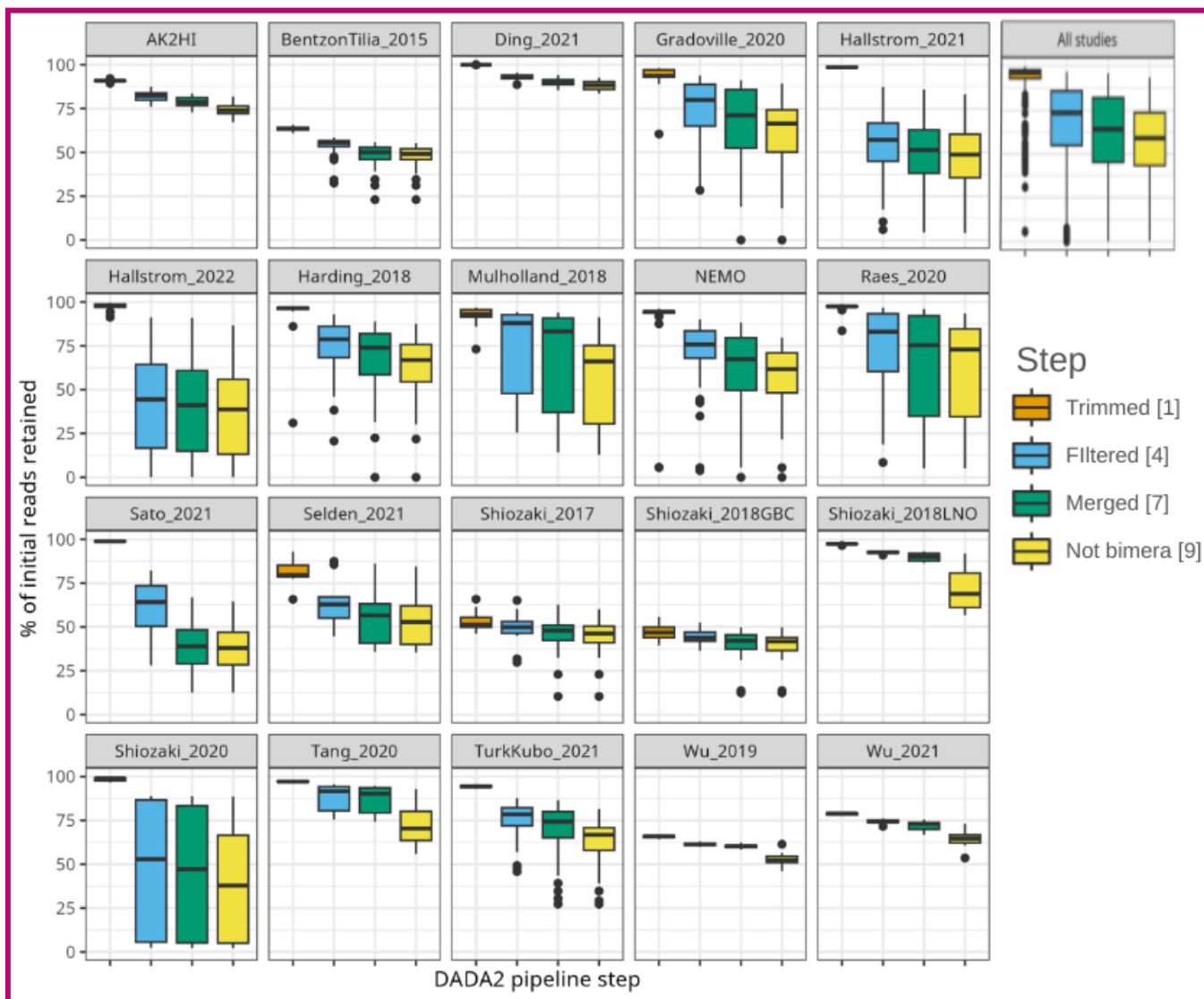
429

430 Interestingly, studies were affected differently by each step of the DADA2 *nifH* pipeline (Fig. 3 and Table 4). There were
 431 major losses of reads during ASV merging, with several studies retaining <2540 % of their total reads by the end of the
 432 pipeline (i.e., ~~BentzonTilia_2015~~, ~~Hallstrom_2022~~, ~~Shiozaki_2020~~, ~~Sato_2021~~, and ~~TianjUni_2016~~ ~~Shiozaki_2020~~), though on
 433 average about half60 % of the reads were retained across studies (Fig. 3 and Table 4).

434



435



436

437 **Figure 3: Study-specific retention of reads at each stage of the pipeline.** The proportion of total reads in each sample that are retained
 438 at the completion of each step of the DADA2 *nifH* pipeline. Each box shows the distribution for samples in the indicated study (using
 439 Study IDs in Table 1), or for all samples together (top right). Proportions for Shiozaki_2017 and Shiozaki_2018GBC reflect that
 440 approximately half the amplicons were not in the orientation expected by the pipeline (see text). Numbers in the legend indicate pipeline
 441 steps in Fig. Figure 1.

442

443 **Table 4: Quality filtering by the DADA2 *nifH* pipeline.** For each study ID are shown the mean numbers of reads retained per sample at
 444 the end of each stage of the DADA2 *nifH* pipeline, as well as the mean percentage of reads retained. Statistics in the bottom three rows
 445 pool all samples. Initial, Trimmed⁴, Filtered⁴, and Merged⁷ and non-Bimera⁹ and their superscripts are specific to the pipeline steps in
 446 Fig. Figure 1. At each step (column) the calculations include only the samples that have >0 reads.

Study	Initial	Trimmed ⁴	Filtered ⁴	Merged ⁹	Non-bimera ⁹	Retained (%)
-------	---------	----------------------	-----------------------	---------------------	-------------------------	--------------

AK2HI	4.5E+04	4.1E+04	3.5E 3.7E+0 4	2.8E 3.6E+0 4	2.8E 3.3E+04	6274.1	
BentzonTilia_2015	8.2E+03	5.3E 5.2E+03	4.6E+03	2.2E 4.1E+0 3	2.1E 4.1E+03	2648.1	
Ding_2021	5.6E+04	5.6E+04	4.8E 5.2E+0 4	4.5E 5.0E+0 4	4.5E 4.9E+04	8288.1	
Gradoville_2020	4.0E+04	3.8E+04	2.9E+04	2.6E+04	2.4E+04	6160.3	
Hallstrom_2021	2.5E+05	2.5E+05	1.5E+05	1.4E+05	1.4E+05	4948.7	
Hallstrom_2022	2.0E+05	1.9E+05	1.0E +05 7.5 E+04	5.4E 7.4E+0 4	4.6E 6.6E+04	1936.3	
Harding_2018	4.2E+04	4.1E+04	3.5E 3.1E+0 4	2.4E 2.9E+0 4	2.3E 2.6E+04	5463.2	
Mulholland_2018	1.8E+05	1.6E+05	1.5E 1.3E+0 5	1.2E+05	1.1E 1.0E+05	6158.5	
NEMO	5.7E+04	5.4E+04	4.6E 4.2E+0 4	3.7E 3.6E+0 4	3.5E 3.3E+04	6057.1	
Raes_2020	9.3E+04	9.1E+04	7.4E 7.7E+0 4	6.6E 6.9E+0 4	6.3E 6.5E+04	6361.0	
Sato_2021	7.5E+04	7.4E+04	4.5E+04	2.9E+04	2.9E+04	3938.8	
Selden_2021	1.5E+05	1.2E+05	9.2E+04	8.2E+04	8.0E+04	5554.7	
Shiozaki_2017	1.8E+04	9.3E+03	8.9E+03	5.8E 8.4E+0 3	5.8E 8.2E+03	2844.1	
Shiozaki_2018GBC	2.4E+04	1.1E+04	1.1E+04	9.2E +03 1.0 E+04	9.1E 9.8E+03	3538.6	
Shiozaki_2018LNO	6.7E+04	6.5E+04	5.6E 6.2E+0 4	3.5E 6.0E+0 4	3.3E 4.8E+04	4971.5	
Shiozaki_2020	2.5E+05	2.5E+05	1.9E 1.8E+0 5	3.4E +04 1.8 E+05	3.3E +04 1.4E+05	1239.1	
Tang_2020	4.7E+04	4.6E+04	3.9E 4.1E+0 4	3.5E 4.0E+0 4	3.2E 3.4E+04	6772.4	
TianjUni_2016 TurkK ubo_2021	8.0E 5.5E+0 4	6.3E 5.2E+04	4.2E+04	3.9E 4.0E+0 4	3.7E 3.6E+04	4663.2	
TianjUni_2017 Wu_20 19	8.0E+04	5.3E+04	2.0E 4.9E+0 4	1.5E 4.8E+0 4	1.4E 4.2E+04	1852.9	
Turk_2021 Wu_2021	5.5E 8.0E+0 4	5.2E 6.3E+04	4.6E 6.0E+0 4	4.0E 5.8E+0 4	3.7E 5.2E+04	6664.4	
All samples	mean	8.9E+04	8.5E+04	6.1E 5.8E+0 4	4.8E 5.4E+0 4	4.5E 4.9E+04	5256.9

and studies	median	5.1E+04	4.8E+04	3.8E3.7E+0	2.9E3.2E+0	2.8E3.0E+04	5659.0
	sum	8.8E+07	8.4E+07	5.9E5.7E+0	4.6E5.3E+0	4.3E4.8E+07	4960.0

447

448

449 ~~Switching the trimming approach from one based on individual read quality profiles (using truncQ in Table 3) to~~
450 ~~fixed-length trimming based on overall quality profiles of the forward and reverse reads (using truncLen.fwd and~~
451 ~~truncLen.rev in Table 2) resulted in more reads being retained for some studies (Sato et al., 2021; Selden et al., 2021;~~
452 ~~Hallström et al., 2022b; Gradoville et al., 2020). However, fixed-length trimming would have required the selection of trim~~
453 ~~lengths based on visual, qualitative assessments of hundreds of FASTQ quality plots which is difficult to accomplish in a~~
454 ~~systematic manner. For consistency we preferred to use nearly identical parameters for most studies (Table 3).~~ ¶

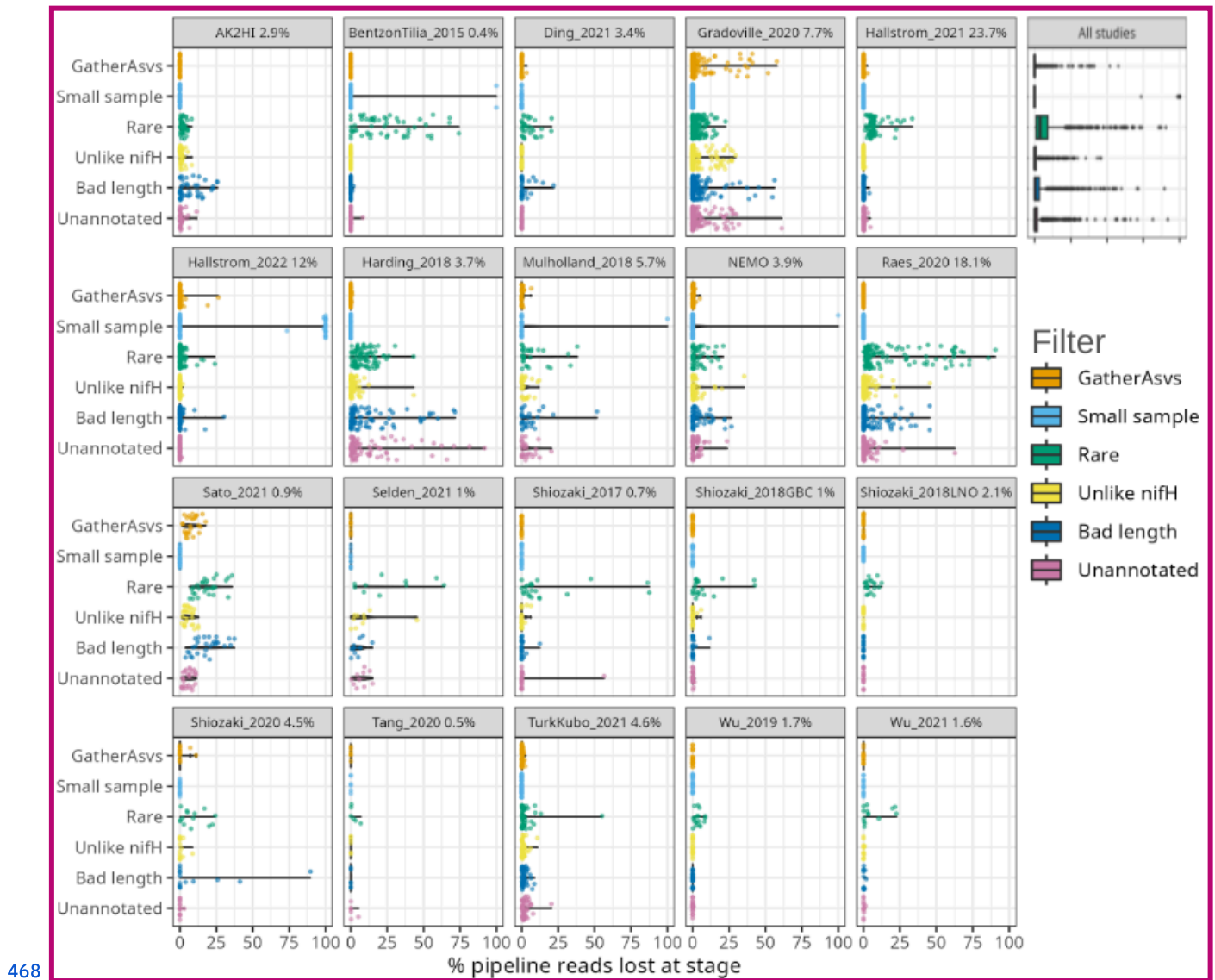
455

456 Post-pipeline stages of the workflow further refined the data (detailed in Methods) (Fig. 4). First, GatherAsvs identified and
457 removed 112163 chimeras using uchime3 denovo (distinct from the bimera filtering done by the pipeline), and then removed
458 818.7 K ASVs that were far outside expected *nifH* lengths (200–450 nt). AUIDs were assigned to the remaining 97139 K
459 unique non-chimeric ASVs (comprising 38.748.4 million total reads; Tables 3 and 5). The GatherAsvs length filter had by
460 far the largest impact of any post-pipeline quality filtering, removing 10 % of the reads from the pipeline. Next, FilterAuids
461 dropped four poorly sequenced samples (7 K total reads), as they would likely misrepresent their diazotrophic communities,
462 and then removed 83 K rare ASVs (2.3 million). FilterAuids stage had the largest impacts on retained data. Thirty-one samples
463 with ≤500 reads were removed because they would likely misrepresent their diazotrophic communities. The FilterAuids
464 rarity check had the greatest reduction to pipeline outputs (121 K ASVs removed and 6.0 % of reads), followed by the length
465 filter (4 K ASVs and 2.7 % of reads; Tables 3 and 5).

466



467



480 Additionally, the last three rows show the overall means, medians, and sums of reads across all samples and studies. Superscripts
 481 correspond to stage numbers in Fig. 1 Post-pipeline stages. The GatherAsvs¹ column mainly reflects length filtering (200–450 nt), and the
 482 WorkspaceStartup⁶ column reflects discarding of ASVs that had no annotation. At each stage (column) the calculations include only the
 483 samples that have >0 reads.

484 ¶

Study ID¶	DADA2¶ pipeline¶	Gather Asvs ¹ ¶	FilterAuids ² ¶			Workspace ⁴ Startup ⁶ ¶	Retained¶ (%)¶	
			Rare¶	Non-NifH¶	Length¶			
AK2HI¶	2.8E+04¶	2.7E+04¶	2.7E+04¶	2.7E+04¶	2.5E+04¶	2.5E+04¶	90¶	
BentzonTilia_2015¶	2.1E+03¶	2.1E+03¶	2.6E+03¶	2.6E+03¶	2.6E+03¶	2.6E+03¶	85¶	
Ding_2021¶	4.5E+04¶	4.5E+04¶	4.2E+04¶	4.2E+04¶	4.1E+04¶	4.1E+04¶	91¶	
Gradoville_2020¶	2.4E+04¶	2.3E+04¶	2.2E+04¶	2.1E+04¶	2.1E+04¶	2.0E+04¶	80¶	
Hallstrom_2021¶	1.4E+05¶	1.4E+05¶	1.3E+05¶	1.3E+05¶	1.2E+05¶	1.2E+05¶	92¶	
Hallstrom_2022¶	4.6E+04¶	2.6E+04¶	3.8E+04¶	3.8E+04¶	3.4E+04¶	3.4E+04¶	50¶	
Harding_2018¶	2.3E+04¶	1.9E+04¶	1.8E+04¶	1.7E+04¶	1.7E+04¶	1.5E+04¶	64¶	
Mulholland_2018¶	1.1E+05¶	9.3E+04¶	9.3E+04¶	9.1E+04¶	8.7E+04¶	8.4E+04¶	72¶	
NEMO¶	3.5E+04¶	3.1E+04¶	3.1E+04¶	3.1E+04¶	3.0E+04¶	3.0E+04¶	80¶	
Raes_2020¶	6.3E+04¶	5.8E+04¶	5.6E+04¶	5.6E+04¶	5.6E+04¶	6.0E+04¶	76¶	
Sato_2021¶	2.9E+04¶	2.7E+04¶	2.1E+04¶	2.0E+04¶	1.5E+04¶	1.4E+04¶	43¶	
Selden_2021¶	8.0E+04¶	8.0E+04¶	6.0E+04¶	5.2E+04¶	4.9E+04¶	4.4E+04¶	52¶	
Shiozaki_2017¶	1.2E+04¶	1.2E+04¶	1.1E+04¶	1.1E+04¶	1.1E+04¶	1.1E+04¶	83¶	
Shiozaki_2018GBC¶	2.0E+04¶	2.0E+04¶	2.0E+04¶	2.0E+04¶	2.0E+04¶	2.0E+04¶	93¶	
Shiozaki_2018LNO¶	3.3E+04¶	3.3E+04¶	3.3E+04¶	3.3E+04¶	3.3E+04¶	3.3E+04¶	92¶	
Shiozaki_2020¶	3.3E+04¶	2.8E+04¶	4.2E+04¶	4.2E+04¶	5.7E+04¶	5.7E+04¶	61¶	
Tang_2020¶	3.2E+04¶	3.0E+04¶	2.9E+04¶	2.9E+04¶	2.9E+04¶	2.9E+04¶	91¶	
TianjUni_2016¶	3.7E+04¶	3.7E+04¶	3.5E+04¶	3.5E+04¶	3.5E+04¶	3.5E+04¶	93¶	
TianjUni_2017¶	1.4E+04¶	1.4E+04¶	1.4E+04¶	1.4E+04¶	1.4E+04¶	1.4E+04¶	96¶	
Turk_2021¶	3.7E+04¶	3.3E+04¶	3.3E+04¶	3.2E+04¶	3.2E+04¶	3.2E+04¶	83¶	
All- samples- and- studies¶	mean¶	4.5E+04¶	4.2E+04¶	4.1E+04¶	4.0E+04¶	4.0E+04¶	4.0E+04¶	79¶
	median¶	2.8E+04¶	2.6E+04¶	2.6E+04¶	2.6E+04¶	2.5E+04¶	2.6E+04¶	90¶
	sum¶	4.3E+07¶	3.9E+07¶	3.6E+07¶	3.6E+07¶	3.5E+07¶	3.4E+07¶	79¶

485

Study ID	DADA2 pipeline	Gather Asvs ¹	FilterAuids ²				Workspace Startup ⁶	Retained (%)
			Small	Rare	Non-NifH	Length		
AK2HI	3.3E+04	3.3E+04	3.3E+04	3.3E+04	3.2E+04	3.0E+04	2.9E+04	89.2
BentzonTilia_2015	4.1E+03	4.1E+03	4.0E+03	3.1E+03	3.1E+03	3.1E+03	3.0E+03	72.8
Ding_2021	4.9E+04	4.9E+04	4.9E+04	4.6E+04	4.6E+04	4.5E+04	4.5E+04	92.2
Gradoville_2020	2.4E+04	2.3E+04	2.3E+04	2.2E+04	2.1E+04	2.1E+04	2.0E+04	82.6

Hallstrom_2021	1.4E+05	1.4E+05	1.4E+05	1.3E+05	1.3E+05	1.2E+05	1.2E+05	92.2	
Hallstrom_2022	6.6E+04	6.5E+04	6.5E+04	6.4E+04	6.4E+04	6.2E+04	6.2E+04	68.1	
Harding_2018	2.6E+04	2.6E+04	2.6E+04	2.4E+04	2.3E+04	2.0E+04	1.7E+04	75.6	
Mulholland_2018	1.0E+05	1.0E+05	1.0E+05	9.5E+04	9.3E+04	8.8E+04	8.4E+04	80.0	
NEMO	3.3E+04	3.3E+04	3.3E+04	3.2E+04	3.2E+04	3.0E+04	3.0E+04	84.2	
Raes_2020	6.5E+04	6.5E+04	6.5E+04	6.1E+04	6.1E+04	6.0E+04	5.9E+04	75.3	
Sato_2021	2.9E+04	2.7E+04	2.7E+04	2.2E+04	2.0E+04	1.5E+04	1.4E+04	49.2	
Selden_2021	8.0E+04	8.0E+04	8.0E+04	6.0E+04	5.2E+04	4.9E+04	4.5E+04	59.0	
Shiozaki_2017	1.6E+04	1.6E+04	1.6E+04	1.5E+04	1.5E+04	1.4E+04	1.4E+04	82.5	
Shiozaki_2018GBC	2.2E+04	2.2E+04	2.2E+04	2.1E+04	2.1E+04	2.1E+04	2.1E+04	90.4	
Shiozaki_2018LNO	4.8E+04	4.8E+04	4.8E+04	4.6E+04	4.6E+04	4.6E+04	4.6E+04	95.0	
Shiozaki_2020	1.4E+05	1.4E+05	1.4E+05	1.4E+05	1.4E+05	1.4E+05	1.4E+05	76.6	
Tang_2020	3.4E+04	3.4E+04	3.4E+04	3.3E+04	3.3E+04	3.3E+04	3.3E+04	97.9	
TurkKubo_2021	3.6E+04	3.5E+04	3.5E+04	3.5E+04	3.5E+04	3.4E+04	3.3E+04	94.1	
Wu_2019	4.2E+04	4.2E+04	4.2E+04	4.1E+04	4.1E+04	4.1E+04	4.1E+04	96.3	
Wu_2021	5.2E+04	5.2E+04	5.2E+04	4.8E+04	4.8E+04	4.8E+04	4.8E+04	93.2	
All samples and studies	mean	5.0E+04	4.9E+04	4.9E+04	4.6E+04	4.6E+04	4.5E+04	4.4E+04	80.9
	median	3.0E+04	3.0E+04	3.0E+04	2.9E+04	2.8E+04	2.7E+04	2.6E+04	93.0
	sum	4.9E+07	4.8E+07	4.8E+07	4.6E+07	4.5E+07	4.4E+07	4.3E+07	90.0

486

487

488 Finally, ASVs were removed if they were classified as non-*nifH*, based on a strong alignment to sequences in NCBI nr that
489 ARBitrator (Heller et al., 2014) classified as non-*nifH*. Specifically, an ASV was classified as non-*nifH* if the ratio of
490 E-values for its best ~~negative and positive~~ **positive and negative** hits, among sequences classified by ARBitrator, was >10. A
491 total of ~~96,095~~ **137,366** of the ~~97,205~~ **139,355** non-chimera ASVs had database hits which resulted in ~~40,448~~ **50,233** positive,
492 ~~12,977~~ **20,528** negative, and ~~42,670~~ **66,605** uncertain classifications. This approach was used to leverage ARBitrator's high
493 specificity for detecting *nifH* as well as to enable users to identify ASVs that have high percent identity matches to sequences
494 in GenBank. An alternative approach would have been to classify the ASVs based on their alignments to HMMs for NifH
495 versus NifH-like proteins (e.g. protochlorophyllide reductase), used by the NifMAP pipeline for *nifH* operational taxonomic
496 units (Angel et al., 2018). Finally, FilterAuids removed ASVs with lengths outside 281–359 nt, a total of ~~974 K reads and~~
497 ~~3063 ASVs~~ **4338 ASVs** comprising **1.2 million reads** (Figs. 1, 4 and Tables 3 and 5). After FilterAUIDs, the total number of
498 samples in the dataset was reduced from 982 to ~~890~~ **951** and the number of ASVs from ~~97,205 to 9416~~ **139,355 to 11,915**.

499

500 FilterAuids also flagged a total of 20002342 ASVs as possible PCR contaminants. Although we opted to flag, not remove,
501 these ASVs, the workflow can be easily altered to remove contaminants. Most studies contained low levels of contamination
502 ($\leq 1\%$) based on our criteria. However, several studies were flagged with $\sim 9\text{--}3029\%$ of their reads being similar to known
503 contaminants. Identifying potential contaminants is challenging given their numerous sources, study specific nature (Zehr et
504 al., 2003), and lack of control sequence data from blanks.

505

506 Next, AnnotateAuids assigned annotations using our three *nifH* reference databases and CART (Fig. 1). In total 79319406 of
507 the 941611,915 quality filtered ASVs were annotated, usually with multiple references (Fig. A1). Most (79269322 ASVs)
508 had hits to both genome879 and ARB2017, likely because the 879 sequenced diazotrophs had *nifH* homologs in GenBank
509 that were found by ARBitrator. Fewer ASVs had hits to the databases that targeted UCYN-A oligos (102217 ASVs) and
510 other marine diazotrophs (645938 ASVs; 96211 ASVs also had UCYN-A hits). Most ASVs (79059380 total) were assigned
511 to NifH clusters 1–4 by CART (respectively, 4100; 79; 36074923; 101; 4205; and 109151 ASVs), including five ASVs that
512 had no hits to our databases. The majority of ASVs (77499257 total) had open reading frames (ORFs) that contained paired
513 cysteines and AMP which might coordinate the 4Fe-4S cluster, and all 77499257 also had annotations from the
514 reference databases or CART. A few ASVs had annotations but lacked residues to coordinate 4Fe-4S: 2329 ORFs lacked the
515 paired cysteines and another 159120 ORFs had paired cysteines but not AMP, usually due to a substitution for M. The last
516 step of AnnotateAuids assigned primary IDs (described above) to 79089383 ASVs. ~~In All of them were retained in the final~~
517 ~~stage of the post-pipeline workflow, WorkspaceStartup retained these 7908 ASVs. One ASV, which had no phylogroup but~~
518 ~~did have paired cysteines and AMP, was also retained. In total the *nifH* ASV database had 7909 ASVs comprising 34.4~~
519 ~~million reads (Table 3(below)).~~

520

521 In the CMAP stage, sample collection metadata (date, latitude, longitude, and depth) were used to download CMAP
522 environmental data (102100 variables) for each sample in the *nifH* ASV database (Fig. 1). The CMAP data will enable
523 analyses of potential factors that influence the global distribution of the diazotrophic community. Aggregated metadata for
524 all samples are available in the *nifH* ASV database (metaTab.csv for sample metadata and cmapTab.csv for environmental
525 data).

526

527 The last stage of the post-pipeline workflow is WorkspaceStartup, which generates the *nifH* ASV database (Fig. 1). ASVs
528 with no annotation are removed as well as samples with zero total reads due to ASV filtering steps. The *nifH* ASV database
529 consisted of 21 studies, 865944 samples, 79099383 AVS and 34.443.0 million total reads (Tables 3 and 5). The database is
530 heavily biased toward euphotic zone DNA samples, with euphotic heuristically defined as follows: Samples were classified
531 as coastal (< 200 km from a major landmass) or open ocean. Euphotic samples were then identified as those collected above
532 a depth cut off, 50 m for coastal samples and 100 m for open ocean. Samples obtained from DNA ($n=768836$) far exceeded
533 those from RNA ($n=94108$) extracts. Likewise, a majority of the samples were from the euphotic zone (789861 compared to

534 7383 from the aphotic zone). The database also includes replicate samples (n=256286) and size fractionated samples
535 (n=142170).

536 3.2 Global *nifH* ASV database

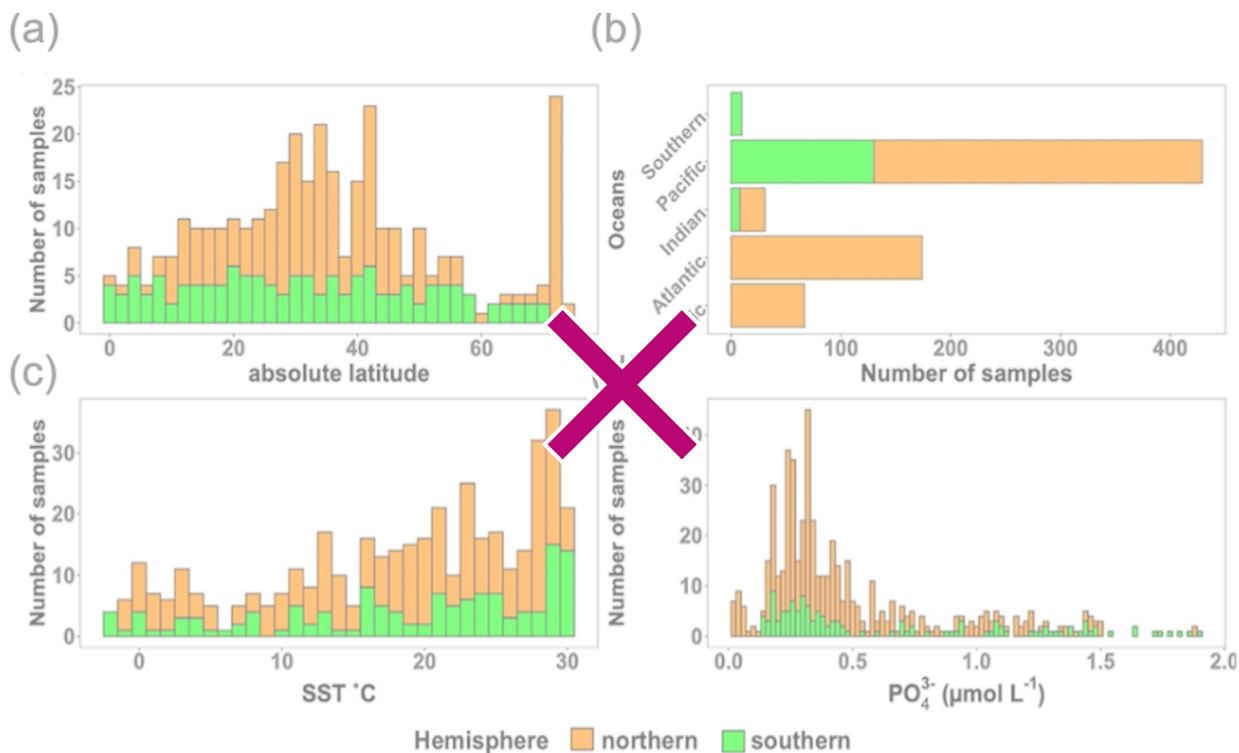
537 3.2.1. Comparison to an OTU database

538 New studies with Illumina amplicon data have mainly used DADA2 (Callahan et al., 2016) and other methods that
539 distinguish fine-scale variation from sequencing errors (Eren et al., 2014; Edgar, 2016b; Amir et al., 2017). Earlier studies,
540 including 13 of the 19 previously published studies in the *nifH* ASV database (Table C1), used *de novo* operational
541 taxonomic units (OTUs) which were obtained by clustering the sequences at 97 % nucleotide identity. OTUs masked
542 sequencing errors as well as fine-scale variation and had other disadvantages compared to ASV approaches (Callahan et al.,
543 2017). Although cross-study comparisons ideally will use the same pipeline for all the studies—the motivation for our
544 workflow—previously published results should be considered. Therefore, for each study in the *nifH* ASV database,
545 diazotroph communities were compared to versions generated using the NifMAP OTU pipeline (Appendix C). The ASV and
546 OTU communities mainly had similar *nifH* clusters, except for several studies where the workflow retained substantially
547 more sequencing reads (Fig. C1, Table C1).

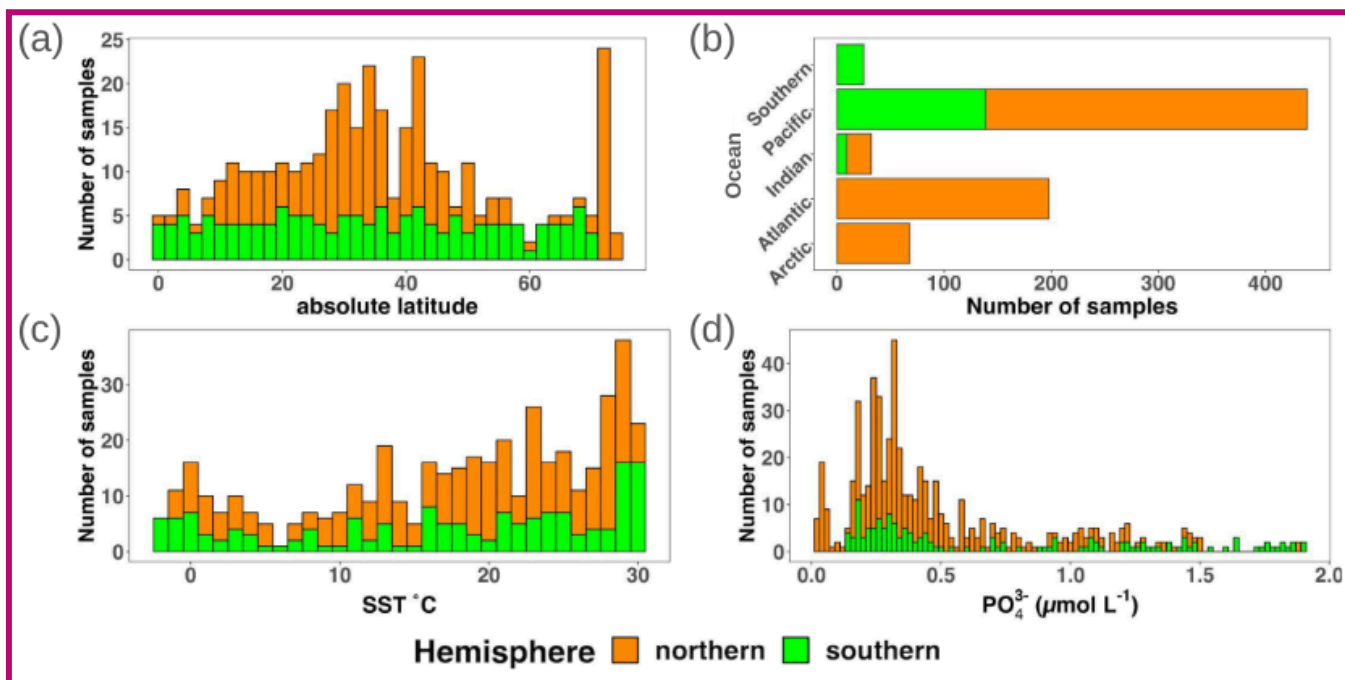
548 3.2.2. Sample Distribution

549 Investigations of N₂ fixation and diazotrophic communities have focused on specific ocean regions and this is reflected by
550 the uneven global distribution of *nifH* amplicon datasets in the *nifH* ASV database (Figs. 2, 5a, and 5b). There is an outsized
551 influence of the northern hemisphere, especially in the Pacific Ocean where most of the database samples were located
552 (429439) and 69.768.3 % of these samples originated from the northern hemisphere (Figs. 2, 5a, 5b, and 6). Ten studies are
553 found within the Pacific, with several containing >50 samples (Figs. 2 and 6). Notably, Raes_2020 (Raes et al., 2020) is the
554 largest dataset stretching from the equator to the Southern Ocean, making up almost the entirety of the southern hemisphere
555 Pacific samples (Figs. 2 and 6). Two new studies carried out in the North Pacific constitute the only previously unpublished
556 data of the *nifH* ASV database (Table 1). AK2HI was a latitudinal transect from Alaska (U.S.) to Hawaii (U.S.) and NEMO
557 was a longitudinal transect across the Eastern North Pacific from San Diego, CA (U.S.) to Hawaii (U.S.) (Fig. 2; Sect. 2.2.2).
558 The amplicon data compiled for the *nifH* ASV database was primarily generated from DNA, with most RNA samples
559 deriving from Atlantic Ocean studies and no contribution from RNA samples in the Arctic or Indian Oceans (Fig. 6).

560



561



562

563 **Figure 5. Location, temperature, and phosphate distributions of the *nifH* ASV**
 564 **database by (a) absolute latitude, (b) the world's oceans, (c) sea surface temperature (SST, °C) and (d) Pisces-derived PO_4^{3-} ($\mu\text{mol L}^{-1}$).**
 565 **Environmental data, (c) and (d), were retrieved from the CMAP data portal.¶**

566 

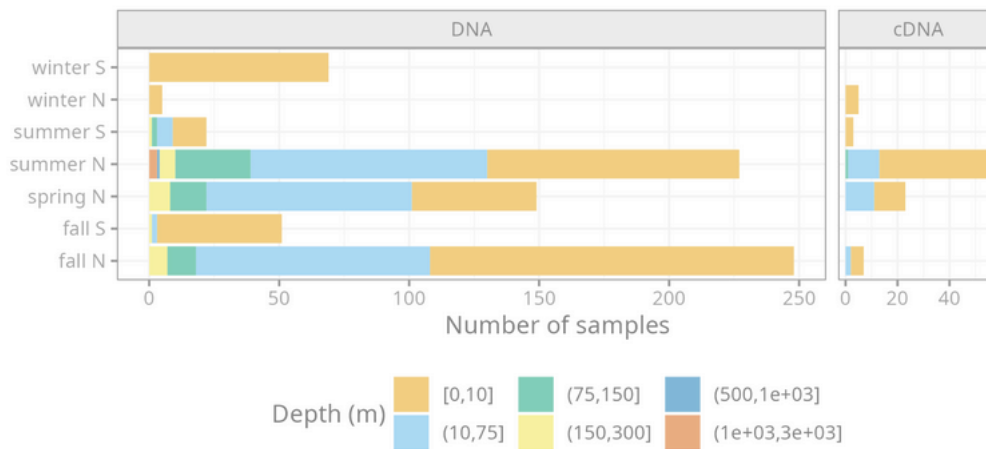
567 All bars are stacked.

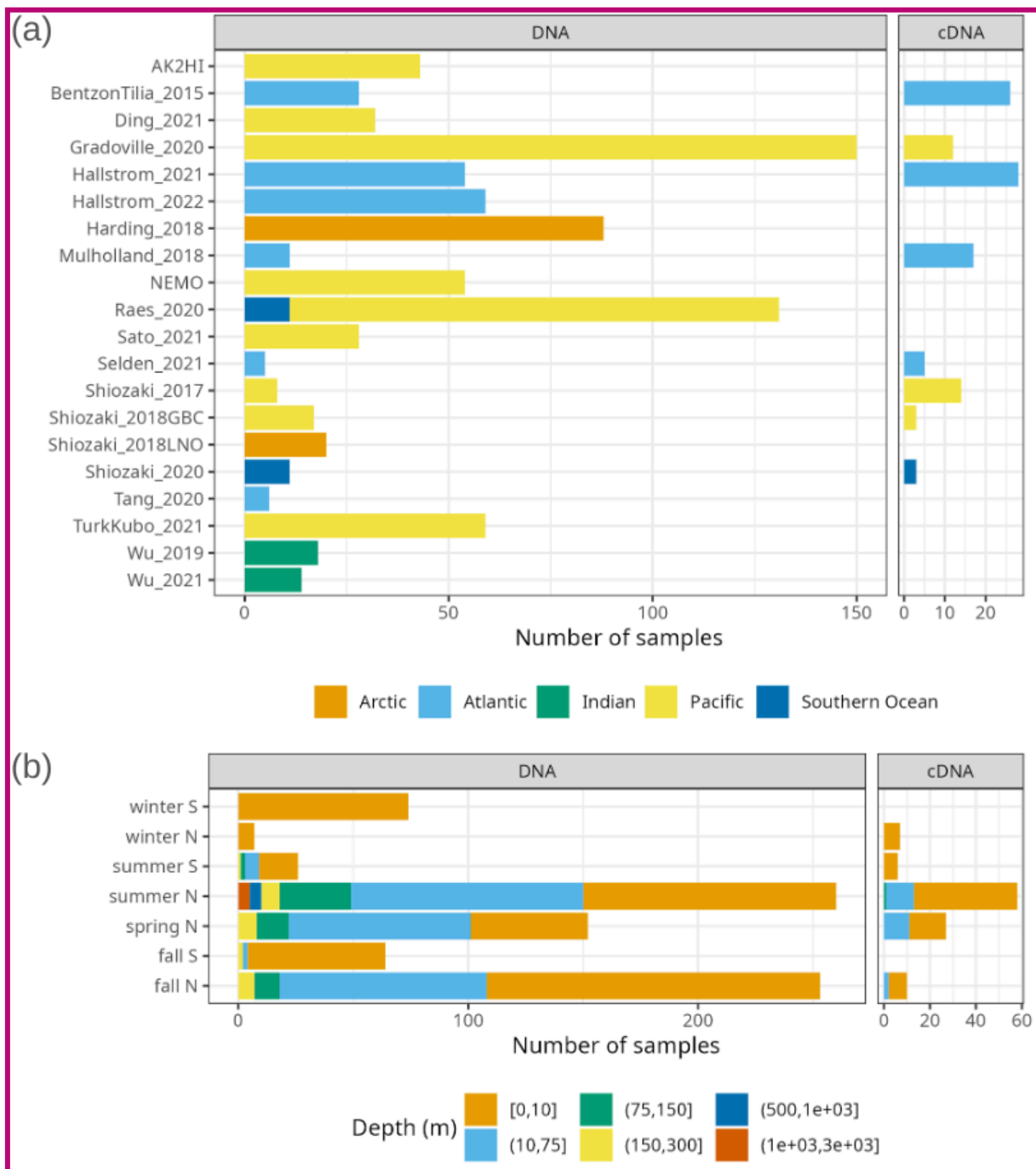
568

(a)



(b)





570
571

572 **Figure 6. Samples in the *nifH* ASV database by collection location, season, and amplicon type.** The number of samples from each
573 study are shown by ocean and study (a), and by the collection season, hemisphere, and depth (b). For both panels the amplicon type (DNA
574 or cDNA) is shown, but x axis scales differ between (a) and (b). See Table 1 for citations for the studies in (a). ~~For (b) there were no~~
575 ~~samples collected between 500—1000 m.~~

576

577

578 Under-sampled regions include the Eastern South Pacific (n=6) and the Western Indian Ocean (n=0) (Figs. 2, 5a, and 6a).
579 Only two studies originated from the Indian Ocean, a unique environment with intense weather and shifting circulation
580 patterns that include monsoon seasons and upwelling conditions that will require much greater sampling coverage to capture
581 diazotroph biogeography. No South Atlantic samples were found during compilation that met the criteria for inclusion in the
582 *nifH* ASV database, though there are several studies from this region (Table A1). Most Atlantic Ocean samples were coastal
583 and from the North Atlantic. Thus, the Atlantic subtropical gyres, which are known to host diverse diazotrophs (Langlois et
584 al., 2005), are underrepresented by *nifH* amplicon data (Fig. 2).

585

586 Tropical and subtropical regions, often associated with high temperatures and low nutrients, are highly represented in the
587 database (Figs. 2 and 5a). This likely influenced the ranges of environmental variables with most samples in the database
588 originating from locations with SST above 15 °C and PO₄³⁻ below 0.5 μmol L⁻¹ (Figs. 5c and 5d). Northern hemisphere
589 samples were collected in all seasons, though fewer from the winter. In contrast, most southern hemisphere samples were
590 collected in the winter and fall (Fig. 6b). While most DNA samples are from the euphotic zone (Fig. 6b), cDNA samples are
591 almost exclusively from the euphotic zone, and mainly from the northern hemisphere during the spring and summer (Fig.
592 6b), indicating an incomplete picture of diazotroph activity.

593

594 The disproportionate spatial and seasonal coverage between hemispheres in the *nifH* ASV database mirrors collection biases
595 in other N₂ fixation metrics including: N₂ fixation rate measurements; diazotroph cell counts; and *nifH* qPCR data, which are
596 heavily sourced from the North Atlantic (Shao et al., 2023) or, when targeting NCDs, also the North Pacific (Turk-Kubo et
597 al., 2022). These biases underscore the need for future work in understudied regions and seasons.

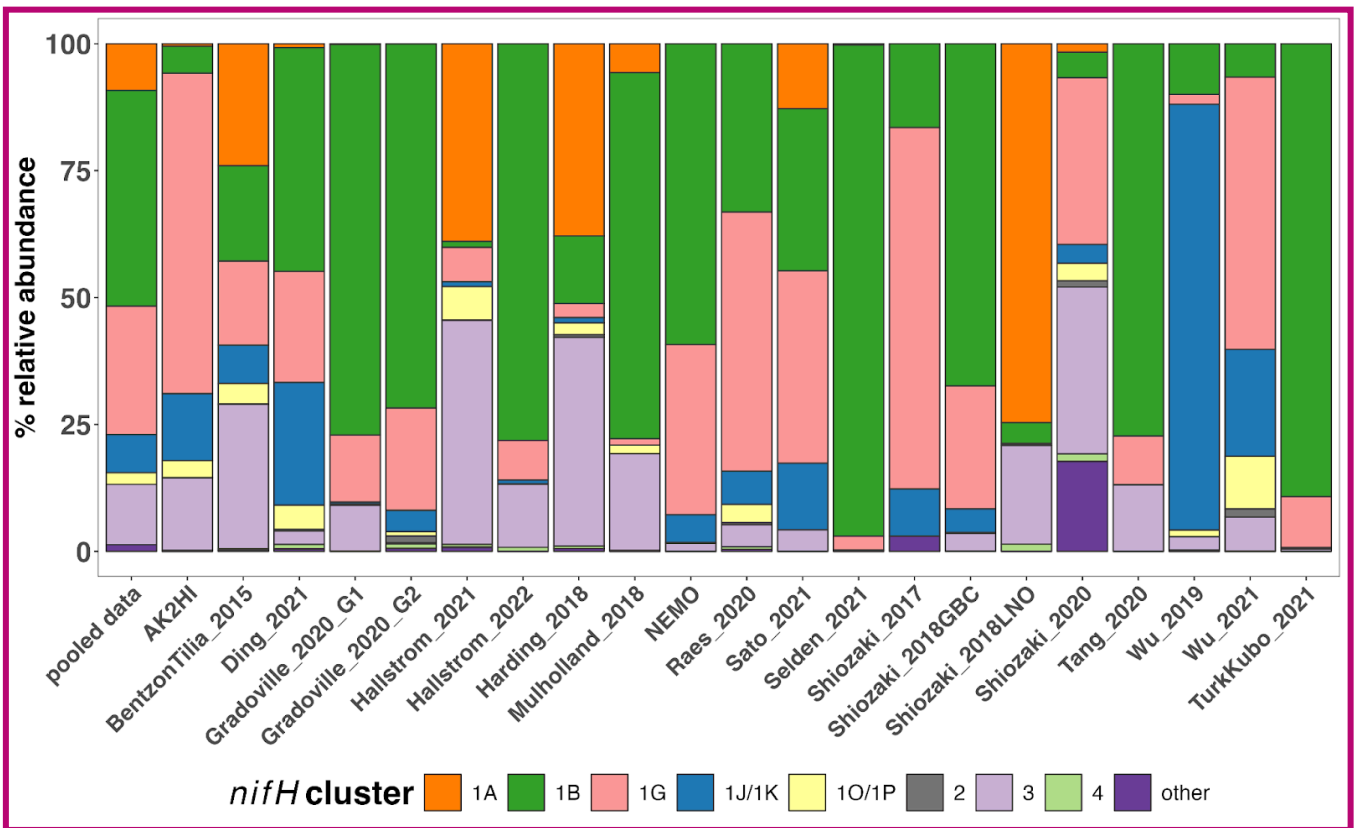
598 3.3 Study-specific patterns in global diazotroph assemblages in the DNA dataset

599 To demonstrate how the *nifH* ASV database can be used, a subset of the data was created that comprised ~~of~~ all DNA samples
600 (~~89.1~~88.8 % of the total dataset; Fig. 7) and referred to herein as the “DNA dataset.” Samples derived from cDNA
601 (n=~~94~~108; Fig. 6) were removed. Replicate samples (n=~~256~~286) or those with multiple size fractions (n=~~142~~170) were
602 combined by averaging across replicates or size fractions. This reduced the number of DNA samples to ~~711~~762 and the total
603 number of reads in the count table to ~~30.0~~36.6 million from ~~34.4~~43.0 million.

604



605



607 **Figure 7. Study-specific diazotroph assemblage patterns in the DNA dataset.** The percentage of (a) total reads and (b) relative
 608 abundance over the DNA dataset for each major *nifH* cluster. The first column of each panel ('pooled data') uses all the compiled data
 609 while each subsequent column only uses data from the indicated study. Colors represent different *nifH* subclusters; 'other' are the
 610 remaining *nifH* clusters.

611

612

613 As demonstrated in a previous global analysis of diazotroph assemblages (Farnelid et al., 2011), cyanobacterial sequences
 614 (cluster 1B) dominate the samples, making up 34 % and 42 % of the total reads and relative abundance, respectively
 615 abundance (Fig. 7). Though photosynthetic cyanobacteria would be expected to thrive in euphotic waters, NCDs are also
 616 widespread in the ocean surface (Langlois et al., 2005; Delmont et al., 2018; Delmont et al., 2022; Pierella Karlusich et al.,
 617 2021; Turk-Kubo et al., 2022). Indeed, among the NCDs, γ -proteobacteria (*nifH* cluster 1G) were the most prevalent,
 618 comprising ca. 23 % of total reads and 27 % of 27 % of the total relative abundance, while δ -proteobacteria (clusters 1A and
 619 3) accounted for 33 % of total reads and 21 % of the total relative abundance of the DNA dataset (Fig. 7). Less prominent
 620 clusters 1J/1K (α - and β -proteobacteria) and 1O/1P (γ -/ β -proteobacteria and Deferribacteres) were ca. 4 % and 6 % of the
 621 reads and 4 % and 3 % of the relative abundance, respectively. The remaining ASVs comprised <1.5 % of the total reads and
 622 relative abundances and came from clusters associated with nitrogenases that do not use iron (e.g. cluster 2) or
 623 that are uncharacterized (cluster 4) (Fig. 7).

624

625 Cluster 1B (cyanobacteria) were generally high in individual studies across the *nifH* DNA dataset, comprising ≥ 25 % of the
626 ~~relative abundance~~ community in two-thirds of the studies (Fig. 7), which is the highest of any cluster. Studies carried out in
627 polar regions (Harding_2018, Shiozaki_2018LNO, Shiozaki_2020) and the Indian Ocean (~~TianjUni_2016~~ and
628 ~~TianjUni_2017~~ Wu_2019 and Wu_2021) were distinct from this pattern, with low relative abundances of cluster 1B. Instead,
629 Arctic studies had high relative abundances of cluster 1A and 3 (both primarily comprised of δ -proteobacteria) and while
630 clusters 1J/1K (α - and β -proteobacteria) and 1O/1P (γ - β -proteobacteria and Deferribacteres) were the
631 ~~predominate~~ predominant groups in the Indian Ocean.

632

633 The second most abundant group was the cluster 1G (γ -proteobacteria), making up ca. 25 % of the total ~~reads~~ relative
634 abundance across the DNA dataset, with study-specific relative abundances greater than 25 % in eight out of 21 studies (Fig.
635 7). Members of this group were often found at high relative abundances in Pacific Ocean studies (AK2HI, NEMO,
636 Raes_2020, Sato_2021, Shiozaki_2017), as well as in other ocean regions including the Atlantic (BentzonTilla_2015), Indian
637 (~~TianjUni_2016~~ Wu_2021) and Southern Ocean (Shiozaki_2020). The notable exception is in Arctic studies; (Harding_2018,
638 Shiozaki_2018LNO) where cluster 1G was almost absent (Fig. 7).

639

640 In several studies, including BentzonTilla_2015, Hallstrom_2021, Mulholland_2018, Selden_2021, Tang_2020, and
641 Hallstrom_2022, diazotroph assemblages had high relative abundances of putative δ -proteobacteria (clusters 1A and 3),
642 reflecting possibly a coastal/shelf or upwelling signature (Figs. 2 and 7). The only study with samples primarily from the
643 Southern Ocean (Shiozaki_2020) was also the only study with a large portion of *nifH* cluster 1E (*Bacillota*).

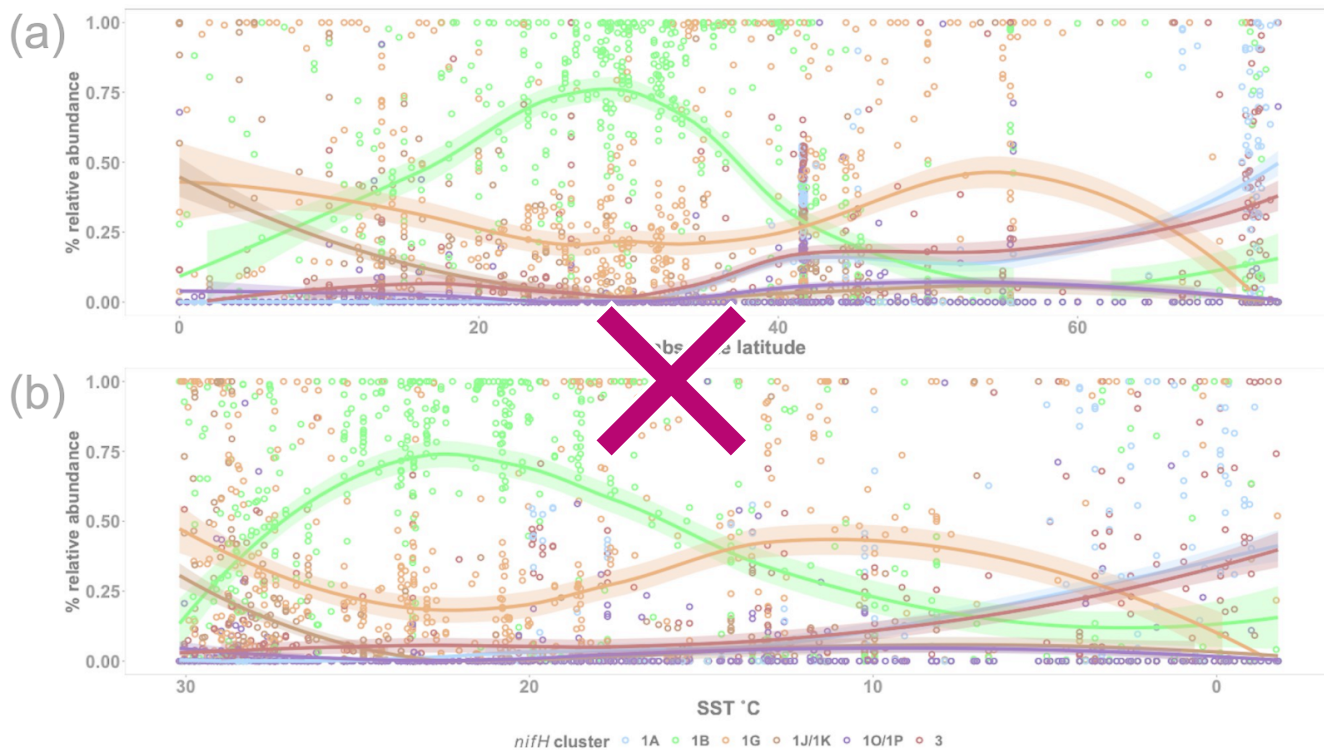
644 3.3.2 Emerging patterns in global diazotroph assemblages across the DNA dataset

645 The *nifH* ASV database enables new analyses of global diazotroph biogeography in the context of environmental parameters,
646 through co-localization with satellite and model outputs publicly available through CMAP (Ashkezari et al., 2021). To
647 demonstrate the utility of the *nifH* ASV database, we present here patterns in relative abundances of *nifH* clusters across
648 absolute latitude and SST in the DNA dataset. Cosmopolitan distributions were evident for γ -proteobacterial (1G) and
649 cyanobacterial diazotrophs (1B; Fig. 8a), corroborating and extending previous findings (Farnelid et al., 2011; Shao and Luo,
650 2022; Halm et al., 2012; Fernandez et al., 2011; Löscher et al., 2014; Cheung et al., 2016). At low to mid latitudes,
651 γ -proteobacterial (1G) diazotrophs generally had high relative abundances and were often the dominant taxa when present.
652 However, they declined within the gyre regions, ranging between ~ 25 –50 % of the population when present, while
653 cyanobacterial diazotrophs (1B) increased and became dominant in the subtropical gyres (Fig. 8a). Notably, cluster 1G
654 diazotrophs reached high relative abundances in each transitional zone, before mainly disappearing at latitudes above 56°
655 (Fig. 8a). However, as mentioned previously, sampling bias likely plays a large role at these higher latitudes where the
656 number of studies and samples are sparse (Figs. 2 and 5).

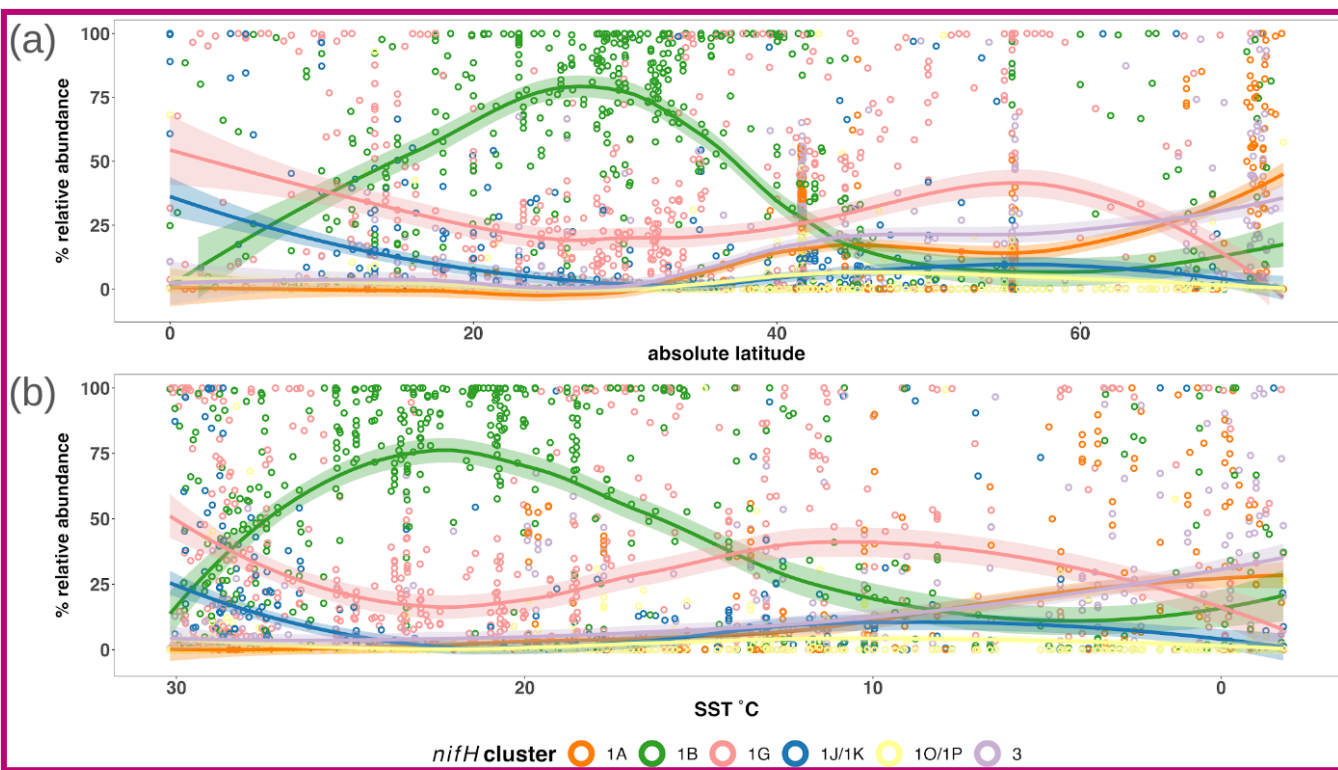
657

658 Clusters 1B and 1G were both detected over the full range of SST (approximately -2–30 °C) but peaks in their relative
659 abundances occurred in distinct SST ranges. Cyanobacterial diazotrophs had multiple peaks in relative abundance in waters
660 >18 °C underscoring their dominance in tropical gyre regions (Fig. 8b). The 1G cluster also spanned the entire temperature
661 spectrum but had notably higher presence and relative abundance above SSTs of 8 °C and 11 °C, respectively (Fig. 8b). The
662 overlap between 1G and 1B has been reported previously, however the factors controlling this are unknown (Moisander et
663 al., 2014; Shiozaki et al., 2017; Shiozaki et al., 2018b; Liu et al., 2020; Tang et al., 2020; Messer et al., 2015).

664



665



666

667 **Figure 8: Global Influence of SST on the global distribution of major *nifH* clusters in the photic zone of the DNA dataset.** The
668 relative abundance of *nifH* genes for each major *nifH* cluster from every photic zone sample compiled in the DNA dataset versus (a)
669 absolute latitudinal latitude and (b) SST. Smoothing averages (lines) were calculated using local polynomial regression fitting (LOESS)
670 with 95 % confidence intervals (translucent colored areas). Each color represents a different *nifH* cluster. SST in (b) is from warmest to
671 coolest temperatures to show that trends are similar to those in (a).

672

673 δ -proteobacterial diazotrophs (clusters 1A and 3) were generally found in cooler, higher latitude waters. Notably, both
674 clusters 1A and 3 were mainly found below $\sim 10^{\circ}\text{C}$ (Fig. 8b). δ -proteobacteria associated with cluster 1A were generally
675 found at latitudes $>32^{\circ}$ and reached maximum relative abundances near the poles, including in the Beaufort Sea, the highest
676 latitude region surveyed (72° ; Figs. 2, 5, and 8a). The vast majority of cluster 1A δ -proteobacteria were found at SST $\leq 5^{\circ}\text{C}$
677 (Fig. 8b). Though cluster 3 and 1A distributions were similar, cluster 3 showed broader spatial and temperature ranges, with
678 consistent but low relative abundances in the subtropics and tropics (Fig. 8).

679

680 In contrast, the relative abundances of cluster 1J/1K and 1O/1P diazotrophs declined as SST decreased and latitude
681 increased, becoming rare at higher latitudes (Fig 8). The highest relative abundances for these clusters were observed near
682 the equator, and in some cases, comprised 100% of the diazotroph assemblage in high SST, tropical samples. These patterns
683 suggest that temperature was an important factor controlling the narrow SST band ($\geq 26^{\circ}\text{C}$) clusters 1J/1K and 1O/1P
684 occupied, establishing them as the *nifH* clusters with the smallest geographic range in the *nifH* ASV database (Fig. 8).

685

686

687 3.4 Limits and caveats to interpreting *nifH* amplicon data

688 The PCR amplification of the *nifH* gene and its transcripts has been vital in advancing the knowledge of diazotroph ecology
689 due to its high sensitivity, detecting diazotrophs at abundances that are often orders of magnitude lower than other marine
690 microbes. This approach has facilitated the discovery of many novel diazotrophs, and provided the first evidence of the
691 widespread distribution of unicellular diazotrophs throughout the open oceans (FalconFalcón et al., 2004; FalconFalcón et
692 al., 2002; Zehr et al., 1998; Zehr et al., 2001). Advances in HTS technologies have revealed diverse diazotrophic
693 assemblages, including the ubiquitously distributed NCDs (Turk-Kubo et al., 2014; Shiozaki et al., 2017; Raes et al., 2020).
694 These discoveries have fostered a new perspective of global diazotrophic ecology (Zehr and Capone, 2020), improved our
695 models of diazotrophic distributions and global N fixation rates (Tang et al., 2019) and will continue to drive new research
696 questions.

697

698 However, interpreting *nifH* PCR-based data requires the consideration of several important caveats. Diazotrophs constitute a
699 small fraction of the total microbial community, and thus often require numerous PCR cycles in conjunction with nested
700 PCR for detection. Increasing the number of cycles can exacerbate known amplification biases (Turk et al., 2011) and

701 increase the likelihood of detecting contaminant sequences (Zehr et al., 2003). Strategies to mitigate and assess
702 contamination exist, e.g., by employing ultrafiltration of reagents and including blanks at different stages of the sampling and
703 sequencing process (Bostrom et al., 2007; Farnelid et al., 2011; Blais et al., 2012; Moisander et al., 2014; Langlois et al.,
704 2015; Fernandez-Mendez et al., 2016; Cheung et al., 2021), but such strategies have not been universally adopted.
705 Additionally, relative abundances of PCR amplicons cannot easily be related to absolute abundances. For example, the
706 relative abundance of a taxon can change even if its absolute abundance remains constant, or the relative abundance can
707 remain constant despite changes in the total assemblage size. Moreover, the complexity of the diazotroph assemblage can, if
708 the HTS sequencing depth is insufficient, cause rare ASVs to go undetected, or have relative abundances which are too low
709 to interpret.

710

711 Primary objectives in studying marine diazotrophic populations include understanding the contribution of each group to N₂
712 fixation, the factors influencing their activity, and their global distributions. The relative abundances of *nifH* genes and
713 transcripts estimated by the workflow can point to potentially significant contributors to N₂ fixation rates. Yet, the presence
714 of *nifH* genes or transcripts does not always correlate with N₂ fixation rates (e.g. (Gradoville et al., 2017)). This underscores
715 the need for cell-specific rates to better constrain N₂ fixation, the assemblages driving given rates, and the taxa-specific
716 regulatory factors of N₂ fixation to better constrain global biogeochemical modeling.

717

718 Various methods are available to target specific diazotroph taxa over space and time (e.g. qPCR/ddPCR, fluorescent in situ
719 hybridization (FISH)-based methods). Universal PCR assays, e.g., those used in the studies compiled here (*nifH*1-4), are an
720 important complement because they better capture the overall diversity of the diazotrophic assemblage. Unlike primers
721 designed for specific sequences, universal primers can amplify unknown or ambiguous sequences, enabling the discovery of
722 genetic diversity. This includes microdiversity, where sequences show subtle variations from known ones, or even
723 identifying entirely novel taxa. Primers specific to novel sequences can then be developed for use in the mentioned
724 quantitative methods, enabling experiments to characterize the growth, activity, and controlling factors/dynamics of putative
725 diazotrophs growth.

726

727 Tools like RT-qPCR, where transcript abundances are assessed directly, or FISH-based methods where single-cells are
728 identified for cell-specific analysis, provide complementary perspectives into the activities of putative diazotrophs.
729 Enumerating diazotrophs using techniques like these can help standardize the relative abundances associated with amplicon
730 sequencing via matching taxa across each method. By assessing diversity and abundance simultaneously, major players can
731 potentially be identified and monitored.

732

733 Through genome reconstruction, omics studies can enhance the characterization of putative diazotroph amplicon sequences
734 by providing a robust suite of associated genetic data, e.g., taxonomic, phylogenetic, and metabolic. Previous studies have

735 led to the assembly of dozens of diazotrophic genomes (Delmont et al., 2022; Delmont et al., 2018). However, omics
736 methods often require massive amounts of data to detect rare community members, and linking genes of interest to other
737 genomic information, e.g., taxonomy, remains quite difficult. Gene-specific models are also required to retrieve diazotrophic
738 information and these models can benefit greatly from the high quality diazotrophic sequences of the *nifH* ASV database. In
739 summary, the complementary perspectives afforded by the methods just described should all be used to obtain robust insights
740 into diazotrophic assemblages.

741

742 **4 Data availability**

743 The *nifH* ASV database is freely available in Figshare (<https://doi.org/10.6084/m9.figshare.23795943.v1v2>; Morando et al.,
744 2024a). HTS datasets for the 21 studies in the database can be obtained from the NCBI Sequence Read Archive using
745 the NCBI BioProject accessions in Table 1.

746 **5 Code availability**

747 The workflow used to generate the *nifH* ASV database is freely available in two GitHub repositories, one for the DADA2
748 *nifH* pipeline (https://github.com/jdmagasin/nifH_amplicons_DADA2; Morando et al., 2024b) and one for the post-pipeline
749 stages (<https://github.com/jdmagasin/nifH-ASV-workflow>; Morando et al., 2024c).

750 **6 Conclusions**

751 The workflow and *nifH* ASV database represent a significant step towards a unified framework that facilitates cross-study
752 comparisons of marine diazotroph diversity and biogeography. Furthermore, they could guide future research, including
753 cruise planning, e.g., focusing more on the southern hemisphere and areas outside of the tropics, and molecular assay
754 development, e.g., assays to characterize NCDs for single-cell activity rates.

755

756 To demonstrate the utility of our framework, the DNA dataset was used to identify potentially important ASVs and
757 diazotrophic groups, establishing global biogeographic patterns from this aggregated amplicon data. Cyanobacteria were the
758 dominant diazotrophic group, but cumulatively the NCDs made up more than half of the total data. Distinct latitudinal
759 patterns were seen among these major diazotrophic groups, with NCDs (clusters 1G, 1J/K, 1O/1P, 1A, and 3) having a
760 greater contribution to relative abundances near the equator and at higher latitudes, while cyanobacteria (1B) comprised a
761 majority of the diazotroph assemblage in the subtropics. SST appeared to restrict and differentiate the biogeography of

762 clusters 1J/1K and 1O/1P (warm tropics/subtropics) from clusters 3 and 1A (cool, high latitude waters), but did not play as
763 large of a role for the biogeography of clusters 1B and 1G.

764

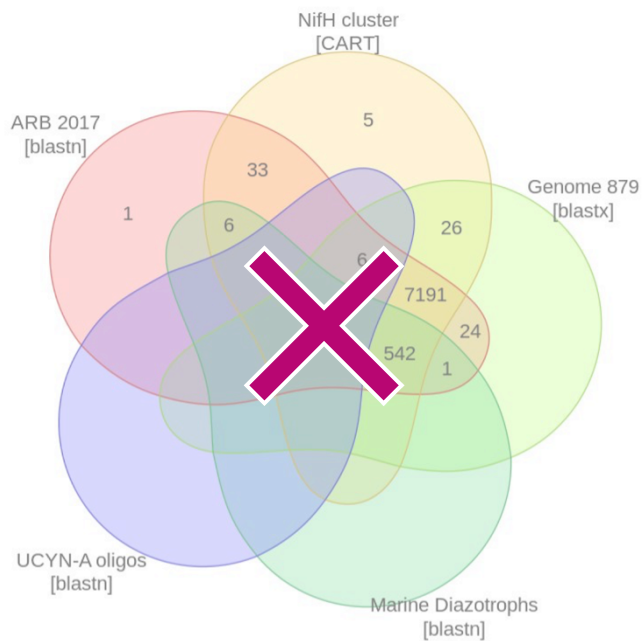
765 We provide the workflow and database for future investigations into the ecological factors driving global diazotrophic
766 biogeography and responses to a changing climate. Ultimately, we hope that insights derived from the use of our framework
767 will inform global biogeochemical models and improve predictions of future assemblages.

768

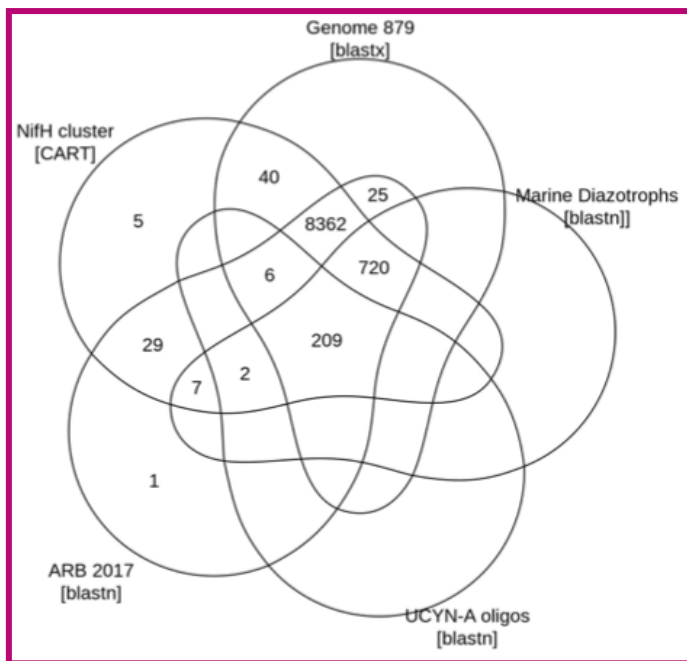
769 **Appendix A:**

770 Figures:

771



772



773

774 **Figure A1. ASV annotations.** The Venn diagram summarizes annotations assigned to 79319406 ASVs during the AnnotateAuids stage of
 775 the workflow (Fig. 1). Numbers indicate how many ASVs received each type of annotation. Of the 941611,915 ASVs from the preceding
 776 workflow stage, FilterAuids, only the 79319406 ASVs shown received annotations.

777

778 Tables:

779 **Table A1. Compiled *nifH* amplicon studies.** Information on all studies compiled to generate the *nifH* ASV database, as well as studies
780 that were not ultimately included and the reasons for this. The table provides the study ID used to refer to each dataset, the NCBI
781 BioProject accession, the number of samples, and the DOI of the publication in which the dataset became public.

Study ID	NCBI BioProject	Sample s	Publication DOI	In <i>nifH</i> ASV-DB?	Reason excluded
AK2HI	PRJNA1062410	43	This study	y	
NEMO	PRJNA1062391	56	This study	y	
Cabello_2020	PRJNA605009	75	10.1111/jpy.13045-20-043	n	Time series samples
Harding_2018	PRJNA476143	91	10.1073/pnas.1813658115	y	
Turk_2021	PRJNA695866	136	10.1038/s43705-021-00039-7	y	
Gradoville_2020_G1	PRJNA530276	111	10.1002/ano.11423	y	
Gradoville_2020_G2	PRJNA530276	56	10.1002/ano.11423	y	
Turk-Kubo_2015	PRJNA300416	11	10.5194/bg-12-7435-2015	n	Mesocosm samples
Farnelid_2019	PRJNA392595	155	10.1002/2017GB005681	n	
Shiozaki_2017	PRJDB5199	22	10.1002/ano.10933	y	
Shiozaki_2018LNO	PRJDB5679	20	10.1038/s41561-020-00651-7	y	
Shiozaki_2020	PRJDB9222	14	10.1029/2017GB005869	y	
Shiozaki_2018GBC	PRJDB6603	20	10.3389/fmicb.2018.00797	y	
Li_2018	PRJNA434503	16	10.1002/ano.10542	n	Issues merging reads
Gradoville_2017	PRJNA328516	49	10.1038/ismej.2014.119	y	
BentzonTilia_2015	PRJNA239310	56	10.3389/fmicb.2017.01122	y	
Gradoville_2017 Frontiers	PRJNA358796	45	10.1038/srep27858	n	Perturbation experiments
Rahav_2016	n/a	n/a	10.1038/s41396-018-0050-z	n	Samples were sorted prior to sequencing
Gerikas-Ribeiro_2018	PRJNA377956	55	10.1038/nmicrobiol.2016.163	n	Samples contained very few sequences
MartinezPerez_2016	PRJNA326820	27	10.1029/2020JC017071	y	
Sato_2021	PRJDB10819	28	10.1002/ano.11727	y	
Selden_2021	PRJNA683637	10	10.1029/2018GB006130	y	
Mulholland_2018	PRJNA841982	29	10.1038/s41598-019-39586-4	y	
MoreiraCoello_2019	PRJNA473903	24	10.1007/s10021-021-00702-z	y	
TianjUni_2016	PRJNA637983	14	10.1007/s00248-019-01355-1	y	
TianjUni_2017	PRJNA438304	18	10.1002/ano.11997	y	
Hallstrom_2021	PRJNA656687	82	10.1007/s10533-022-00940-w	y	
Hallstrom_2022	PRJNA756869	83	10.3389/fmars.2020.00389	y	
Raes_2020	PRJNA385736	121	10.1038/s41396-020-0703-6	y	
Tang_2020	PRJNA554315	6	10.3390/biology10060555	y	
Ding_2021	SUB7406573	32	10.1007/s13131-019-1513-4	y	

782 *: Data were obtained from authors, not the SRA.

Study ID	Sam ples	NCBI BioProject	Reference	DOI	In <i>nifH</i> ASV database?
AK2HI	43	PRJNA1062410	This study	n/a	Yes
BentzonTilia_2015	56	PRJNA239310	Bentzon-Tilia et al., 2015	10.1038/ismej.2014.119	Yes
Cabello 2020	75	PRJNA605009	Cabello et al., 2020	10.1111/jpy.13045	No. Time series samples
Ding_2021	32	SUB7406573	Ding et al., 2021	10.3390/biology10060555	Yes

Farnelid 2019	155	PRJNA392595	Farnelid et al., 2019	10.1038/s41396-018-0259-x	No. Particle enrichment samples
Gérikas Ribeiro 2018	55	PRJNA377956	Gérikas Ribeiro et al., 2018	10.1038/s41396-018-0050-z	No. Samples had very few sequences
Gradoville 2017 Frontiers	45	PRJNA358796	Gradoville et al., 2017	10.3389/fmicb.2017.01122	No. Perturbation experiments
Gradoville_2020_G1	111	PRJNA530276	Gradoville et al., 2020	10.1002/lno.11423	Yes
Gradoville_2020_G2	56	PRJNA530276	Gradoville et al., 2020	10.1002/lno.11423	Yes
Hallstrom_2021	82	PRJNA656687	Hallstrøm et al., 2022b	10.1002/lno.11997	Yes
Hallstrom_2022	83	PRJNA756869	Hallstrøm et al., 2022a	10.1007/s10533-022-00940-w	Yes
Harding_2018	91	PRJNA476143	Harding et al., 2018	10.1073/pnas.1813658115	Yes
Li 2018	16	PRJNA434503	Li et al., 2018	10.3389/fmicb.2018.00797	No. Issues merging reads
Mulholland_2018	29	PRJNA841982	Mulholland et al., 2019	10.1029/2018GB006130	Yes
NEMO	56	PRJNA1062391	This study	n/a	Yes
Raes_2020	121	PRJNA385736	Raes et al., 2020	10.3389/fmars.2020.00389	Yes
Rahav 2016	n/a	n/a	Rahav et al., 2016	10.1038/srep27858	No. Samples sorted prior to sequencing
Sato_2021	28	PRJDB10819	Sato et al., 2021	10.1029/2020JC017071	Yes
Selden_2021	10	PRJNA683637	Selden et al., 2021	10.1002/lno.11727	Yes
Shiozaki_2017*	22	PRJDB5199	Shiozaki et al., 2017	10.1002/2017GB005681	Yes
Shiozaki_2018GBC*	20	PRJDB6603	Shiozaki et al., 2018b	10.1029/2017GB005869	Yes
Shiozaki_2018LNO	20	PRJDB5679	Shiozaki et al., 2018a	10.1002/lno.10933	Yes
Shiozaki_2020	14	PRJDB9222	Shiozaki et al., 2020	10.1038/s41561-020-00651-7	Yes
Tang_2020	6	PRJNA554315	Tang et al., 2020	10.1038/s41396-020-0703-6	Yes
Turk-Kubo 2015	11	PRJNA300416	Turk-Kubo et al., 2015	10.5194/bg-12-7435-2015	No. Mesocosm samples
TurkKubo_2021	136	PRJNA695866	Turk-Kubo et al., 2021	10.1038/s43705-021-00039-7	Yes
Wu_2019	18	PRJNA438304	Wu et al., 2019	10.1007/s00248-019-01355-1	Yes
Wu_2021*	14	PRJNA637983	Wu et al., 2021	10.1007/s10021-021-00702-z	Yes

783

784

785 Appendix B: Read trimming method effects on workflow outputs

786 It is well-established that error rates increase with the number of PCR cycles during Illumina sequencing (Manley et al.,
787 2016). DADA2 trims the reads to remove the low-quality tails, an important early step that impacts the proportion of
788 sequences retained during quality-filtering and merging, as well as the ASVs detected (Fig. 1). Usually sequencing quality
789 plots are inspected to identify a trimming length that will on average cut the reads before quality declines significantly.
790 However, inspecting tens to hundreds of quality plots (depending on the study size) is laborious and unsystematic. For the
791 present work, the pipeline ancillary script estimateTrimLengths.R was used to efficiently identify lengths that maximized the

792 percentages of reads retained for each study (Section 2.3.2). The optimized lengths appeared in the parameter files as
793 `truncLen.fwd` and `truncLen.rev` used by DADA2 `filterAndTrim` (Table 2).

794

795 An alternative to fixed-length trimming is to trim each read based on its individual quality profile, at the first position where
796 the estimated sequencing error rate exceeds a threshold specified in the `truncQ` parameter to `filterAndTrim` (Table 2). This
797 approach might reduce mismatches in the overlapping regions during the merge step and thus retain more read pairs.
798 However, spurious low-quality bases could cause overly aggressive trimming, and picking a threshold that allows most
799 sequences to overlap is not straightforward.

800

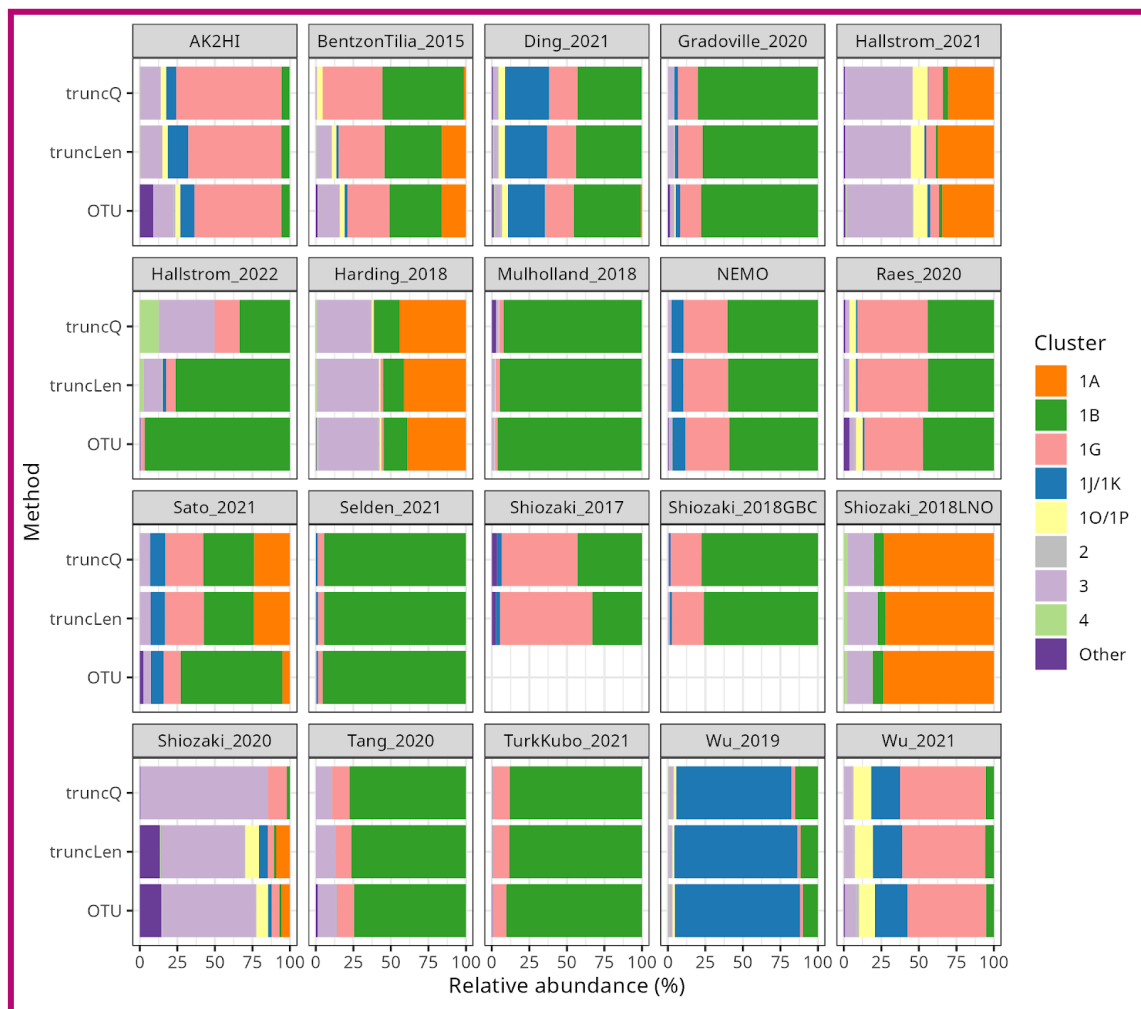
801 The quality of the raw sequencing data is a critical factor in the generation of the final ASV table. When analyzing a new
802 dataset, testing both the fixed-length (`truncLen`) and quality-based (`truncQ`) trimming methods is suggested because they are
803 fundamentally different and `filterAndTrim` impacts all downstream DADA2 steps. If both methods produce similar ASVs
804 and abundances, additional parameter tuning is unlikely to impact the analysis meaningfully.

805

806 To illustrate how the trimming approach can impact workflow outputs, a version of the *nifH* ASV database was generated as
807 shown in Figure 1 except that reads were trimmed at the first position where the estimated error rate was $>2.5\%$ (`truncQ =`
808 `16` in Table 2). This threshold typically produces forward and reverse ASVs of sufficient length to overlap without
809 mismatches. The `truncQ` version of the database had substantially fewer samples, reads, and ASVs (Table B1), partly
810 because `truncQ` appeared more affected by low quality reads (discussed below). Only 1783 ASVs out of 9383 in the *nifH*
811 ASV database were detected by both trimming methods, but they comprised 88.3 % of the total reads in the database (Table
812 B1). The 7600 ASVs (16.7 % of reads) that were found only using `truncLen` had mainly low abundances and were detected
813 mainly in one to several samples. Although `truncQ` was less sensitive to rare ASVs, for most studies the relative abundances
814 of *nifH* groups were similar using either trimming approach (Fig. B1).

815

816 There were three exceptions where sequencing quality issues caused substantial differences in the results from `truncQ` and
817 `truncLen`, `BentzonTilia_2015`, `Hallstrom_2022`, and `Shiozaki_2020`. Using either trimming method, all three studies lost
818 high percentages of reads during `filterAndTrim` (Fig. 3; losses using `truncQ` were comparable). This indicates that
819 sequencing errors remained after trimming (>2 errors in the trimmed forward reads and >4 in the reverse; `maxEE` in Table 2).
820 However, the subsequent losses during `mergePairs` were much higher using `truncQ` (vs. `truncLen`), respectively 58 % (10 %),
821 61 % (5 %), and 72 % (6 %) of reads. This suggests that trimming with `truncQ=16` more frequently produced reads that
822 failed to overlap during the merge step. For these three studies the workflow discarded many samples due to having ≤ 500
823 reads, but more with `truncQ` (vs. `truncLen`), respectively $n=54$ (34); 59 (29); and 14 (5) samples discarded. These three
824 exceptions suggest that `truncLen`-based trimming can retain substantially more reads and samples for FASTQs with lower
825 quality reads, which could impact relative abundances (Fig. B1).



828

829 **Figure B1. Relative abundances using different DADA2 trimming methods and the NifMAP OTU pipeline.** *nifH* cluster relative
 830 abundances are shown for each study when processed using the NifMAP OTU pipeline (Angel et al., 2018) or by the *nifH* workflow using
 831 two methods for trimming reads, quality-based (truncQ) or fixed-length (truncLen). ASV or OTU abundances for the samples in a study
 832 were pooled to calculate the relative abundances shown. The three results for each study were calculated using only the samples that were
 833 retained by both runs of the *nifH* workflow. Shiozaki_2017 and Shiozaki_2018GBC used mixed-orientation sequencing libraries and could
 834 not be processed by NifMAP.

835

836 [Tables:](#)

837 **Table B1. Impact of read trimming method on workflow outputs.** The table compares the *nifH* ASV database, generated using
 838 fixed-length read trimming (truncLen for DADA2 filterAndTrim), to an alternative database for which reads were trimmed at the first
 839 nucleotide where the error rate was >2.5 % (truncQ=16). No other pipeline or post-pipeline parameters were changed.

840

	truncLen	truncQ	% decrease
--	----------	--------	------------

Samples	944	847	10.4
ASVs	9383	1997	78.7
Reads	43.0E+6	26.3E+6	38.9

841

842

843 **Appendix C: Comparison of communities from the workflow to previous studies**

844 Prior to DADA2 (Callhan et al. 2016) and other approaches that distinguish fine-scale variation from sequencing errors
845 (Eren et al. 2014, Edgar 2016b, Amir et al. 2017), most amplicon studies—for 16S rRNA as well as functional
846 genes—processed their sequencing data into operational taxonomic units (OTUs). Usually this meant *de novo* clustering the
847 amplicon sequences at 97 % nucleotide identity and using a representative sequence from each of the OTUs (clusters) for
848 subsequent analyses. For 16S rRNA genes, it is known that PCR artifacts and sequencing errors can inflate the number of
849 OTUs and cause diversity to be overestimated (Quince et al., 2009; Eren et al., 2013). For *nifH* amplicon data, these issues
850 have been mitigated in previously published OTU analyses by analyzing broad diazotroph groups (Table C1).

851

852 To demonstrate whether communities derived from the workflow differ substantially from those previously published, a
853 comparison was made between the results from the *nifH* workflow and another *nifH* pipeline, NifMAP (Angel et al. 2018).
854 NifMAP is an OTU pipeline that uses hidden Markov models in an attempt to distinguish true *nifH* sequences from orthologs
855 often mistaken for *nifH*. NifMAP was used to generate proxies for most of the 21 studies since complete OTU sequences and
856 abundances were not available for the 19 original studies. Using NifMAP for all studies was more systematic than trying to
857 reproduce the original results which depended on different software and methods for quality filtering. Additionally, the
858 workflow and NifMAP both use CART (Frank et al. 2016) to identify *nifH* clusters enabling the cross-comparison of major
859 *nifH* groups. Both also distinguish *nifH* from orthologs, the workflow using `classifyNifH.sh` described in section 2.3.3). Only
860 the samples that were processed by both the workflow and NifMAP were compared (n=902).

861

862 The main result was that similar diazotroph communities were detected by the *nifH* workflow and NifMAP (Fig. B1). For
863 every study they agreed on the two most abundant *nifH* subclusters, usually with ≤ 3 % difference between the relative
864 abundances from the workflow and NifMAP. These results suggest that comparisons between new and previously published
865 *nifH* amplicon studies are possible, especially if both use similarly broad taxonomic levels, e.g., *nifH* subclusters.

866

867 However, for two studies there were clear differences between the *nifH* workflow and NifMAP that speak to the utility of the
868 workflow. For Hallstrom_2022 the workflow detected additional *nifH* subclusters, mainly 3 and 1G, and for Sato_20201 the
869 workflow detected 1G and 1A at much higher levels (Fig. B1). These compositional differences likely stemmed from vastly
870 greater numbers of reads retained by the workflow compared to NifMAP (1034 % and 264 % more reads, respectively for
871 the two studies; Table C1). The NifMAP logs revealed that poor read quality caused NifMAP to discard the majority of reads

872 in the first two steps. Only 10% of the Hallstrom_2022 reads could be merged, the lowest of any study (median 78 %, range
873 10–94 %), and 56 % of the reads from Sato_2021. The merged reads were short for both Hallstrom_2022 (mean 174 nt) and
874 Sato_2021 (198 nt) in comparison to all studies (median of 307 nt). NifMAP then discarded, respectively, 66 % and 58 % of
875 the merged reads due to lengths < 200 nt. In comparison, for Hallstrom_2022 the workflow discarded most reads during
876 DADA2 filterAndTrim (using truncLen) due to sequencing errors but discarded few reads during mergePairs (Fig. 3 and
877 Table 4). This suggests that DADA2 denoising worked very well for this dataset because the forward and reverse ASVs were
878 allowed at most one mismatch in their overlapping region (Table 2). In contrast, Sato_2021 had substantial losses of reads
879 during both filterAndTrim and mergePairs (Fig. 3 and Table 4). Together these results indicate that the *nifH* workflow can
880 potentially retain more reads than NifMAP, particularly when data quality is low, with noticeable impacts on community
881 composition.

882

883 Although community compositions from the workflow and NifMAP were mainly similar (Fig. B1), the workflow tended to
884 retain more of the sequencing reads (Table C1). For 9 of the 18 studies analyzed by both the workflow and NifMAP, there
885 was <10 % difference in the number of reads retained into final sequences (ASVs or OTUs; Table C1). However, 6 of the
886 other 9 studies had more reads retained by the workflow (14–1034 %) and 3 had more reads retained by NifMAP (10–23 %).
887 Although the workflow retained more reads, usually there were fewer ASVs than OTUs despite compression from clustering
888 at 97 % nucleotide identity (Table C1). This is consistent with the known limitations of OTUs mentioned earlier, errors and
889 overestimated diversity.

890

891

892 Tables:

893

894 **Table C1.** Summary of the total reads and final sequences obtained by the workflow (ASVs) and NifMAP (OTUs) applied to the same
895 samples. A total of 902 of 944 samples in the *nifH* ASV database were compared. This excludes 42 samples from Shiozaki_2017 and
896 Shiozaki_2018GBC that used mixed-orientation sequencing libraries and could not be processed by NifMAP. The Change (%) column is
897 relative to reads in OTUs. OTUs in column 6 count clusters (97 % nucleotide identity). *: The original publication analyzed OTUs.
898

Study ID	Samples compared	Reads (K)			Sequences	
		In OTUs	In ASVs	Change (%)	OTUs	ASVs
AK2HI	43	1319	1259	4.6	987	283
BentzonTilia_2015*	54	220	171	22.6	1043	352
Ding_2021*	32	1358	1446	-6.5	1362	435
Gradoville_2020 (G1,G2)*	162	3200	3304	-3.3	642	333
Hallstrom_2021	82	4531	10,216	-125.5	14,606	6403
Hallstrom_2022*	59	455	5155	-1033.8	91	165

Harding_2018*	88	1384	1579	-14.1	1715	842
Mulholland_2018	28	2527	2439	3.5	1706	549
NEMO	54	1830	1665	9.0	591	177
Raes_2020	131	7668	7793	-1.6	1421	395
Sato_2021	28	106	388	-264.1	141	169
Selden_2021	10	405	445	-9.9	217	60
Shiozaki_2018LNO*	20	618	913	-47.8	929	283
Shiozaki_2020	14	946	1935	-104.7	1664	123
Tang_2020*	6	229	196	14.2	235	35
TurkKubo_2021*	59	2011	1976	1.8	305	74
Wu_2019*	18	801	734	8.3	504	102
Wu_2021*	14	749	674	10.0	1315	180

899

900

901 Author Contributions

902 KTK and MM designed the study with input from SC and MMM. JM created and optimized the DADA2 pipeline for *nifH*
903 amplicon analyses. JM and MM developed the post-pipeline workflow. MM and JM compiled the database, retrieved
904 environmental data from CMAP, and analyzed the database. MM, JM and KTK wrote the manuscript with input from
905 MMM, SC, and JPZ.

906 Competing Interests

907 No competing interest is declared.

908 Acknowledgements

909 We gratefully acknowledge Mohammad Ashkezari and the Simons CMAP team, Stefan Green (Rush University) and the
910 DNA genomics core at University of Illinois at Chicago, Irina Shilova, Julie Robidart and Grace Reed for NEMO sampling
911 and sample processing, and Angelicque White (University of Hawaii, Manoa) and Mary R. Gradoville (Columbia River
912 Inter-Tribal Fish Commission) for AK2HI sampling and sample processing. We would like to thank the authors who directly
913 provided access to sequences: Takuhei Shiozaki (Shiozaki_2017 and Shiozaki_2018GBC) and Jun Sun, Changling Ding, and
914 Chao Wu (TianjUni_2016Wu_2021). This work was supported by grants from the National Science Foundation to KTK

915 (OCE-2023498) and the Simons Foundation to JPZ (Simons Collaboration on Ocean Processes and Ecology, Award ID
916 724220).
917

918 **References**

- 919 Amir, A. McDonald, D., Navas-Molina, J. A., Kopylova, E., Morton, J. T., Zech Xu, Z., Kightley, E. P., Thompson, L. R.,
920 Hyde, E. R., Gonzalez, A., and Knight, R.: Deblur rapidly resolves single-nucleotide community sequence patterns,
921 *mSystems*, 2, 10.1128/msystems.00191-16, 2017.
- 922 Angel, R., Nepel, M., Panholzl, C., Schmidt, H., Herbold, C. W., Eichorst, S. A., and Woebken, D.: Evaluation of Primers
923 Targeting the Diazotroph Functional Gene and Development of NifMAP - A Bioinformatics Pipeline for Analyzing nifH
924 Amplicon Data, *Front Microbiol*, 9, 703, 10.3389/fmicb.2018.00703, 2018.
- 925 Ashkezari, M. D., Hagen, N. R., Denholtz, M., Neang, A., Burns, T. C., Morales, R. L., Lee, C. P., Hill, C. N., and Armbrust,
926 E. V.: Simons Collaborative Marine Atlas Project (Simons CMAP): An open-source portal to share, visualize, and analyze
927 ocean data, *Limnol. Oceanogr.: Methods*, 19, 488-496, 2021.
- 928 Benavides, M., Conradt, L., Bonnet, S., Berman-Frank, I., Barrillon, S., Petrenko, A., and Doglioli, A.: Fine-scale sampling
929 unveils diazotroph patchiness in the South Pacific Ocean, *ISME Communications*, 1, 3, 2021.
- 930 Bentzon-Tilia, M., Traving, S. J., Mantikci, M., Knudsen-Leerbeck, H., Hansen, J. L. S., Markager, S., and Riemann, L.:
931 Significant N₂ fixation by heterotrophs, photoheterotrophs and heterocystous cyanobacteria in two temperate estuaries, *ISME*
932 *J*, 9, 273-285, 2015.
- 933 Blais, M., Tremblay, J. É., Jungblut, A. D., Gagnon, J., Martin, J., Thaler, M., and Lovejoy, C.: Nitrogen fixation and
934 identification of potential diazotrophs in the Canadian Arctic, *Global Biogeochem. Cy.*, 26, GB3022,
935 10.1029/2011gb004096, 2012.
- 936 Bostrom, K. H., Riemann, L., Kuhl, M., and Hagstrom, A.: Isolation and gene quantification of heterotrophic N₂-fixing
937 bacterioplankton in the Baltic Sea, *Environ. Microbiol.*, 9, 152-164, doi:10.1111/j.1462-2920.2006.01124.x, 2007.
- 938 Cabello, A. M., Turk-Kubo, K. A., Hayashi, K., Jacobs, L., Kudela, R. M., and Zehr, J. P.: Unexpected presence of the
939 nitrogen-fixing symbiotic cyanobacterium UCYN-A in Monterey Bay, California, *J Phycol*, 56, 1521-1533,
940 10.1111/jpy.13045, 2020.
- 941 Callahan, B. J., McMurdie, P. J., Rosen, M. J., Han, A. W., Johnson, A. J., and Holmes, S. P.: DADA2: High-resolution
942 sample inference from Illumina amplicon data, *Nat Methods*, 13, 581-583, 10.1038/nmeth.3869, 2016.
- 943 Callahan, B.J., McMurdie, P. J., and Holmes, S. P.: Exact sequence variants should replace operational taxonomic units in
944 marker-gene data analysis, *ISME J*, 11, 12, 2639–2643, 2017.
- 945 Capone, D. G., Burns, J. A., Montoya, J. P., Subramaniam, A., Mahaffey, C., Gunderson, T., Michaels, A. F., and Carpenter,
946 E. J.: Nitrogen fixation by *Trichodesmium* spp.: An important source of new nitrogen to the tropical and subtropical North
947 Atlantic Ocean, *Global Biogeochem. Cy.*, 19, GB2024: 2021-2017, 2005.
- 948 Carpenter, E. J. and Capone, D. G.: Nitrogen in the marine environment, Academic Press, New York, 900 pp.1983.

- 949 Carpenter, E. J. and Foster, R. A.: Marine symbioses, in: *Cyanobacteria in Symbiosis*, edited by: Rai, A. N., Bergman, B.,
950 and Rasmussen, U., Kluwer Academic Publishers, The Netherlands, 11-18, 2002.
- 951 Cheung, S., Xia, X., Guo, C., and Liu, H.: Diazotroph community structure in the deep oxygen minimum zone of the Costa
952 Rica Dome, *J Plankton Res*, 38, 380-391, 2016.
- 953 Cheung, S., Zehr, J. P., Xia, X., Tsurumoto, C., Endo, H., Nakaoka, S. I., Mak, W., Suzuki, K., and Liu, H.: Gamma4: a
954 genetically versatile Gammaproteobacterial *nifH* phylotype that is widely distributed in the North Pacific Ocean, *Environ*
955 *Microbiol*, 23, 4246-4259, 10.1111/1462-2920.15604, 2021.
- 956 Coale, T. H., Loconte, V., Turk-Kubo, K. A., Vanslebrouck, B., Mak, W. K. E., Cheung, S., Ekman, A., Chen, J. H.,
957 Hagino, K., Takano, Y., Nishimura, T., Adachi, M., Le Gros, M., Larabell, C., and Zehr, J. P.: Nitrogen-fixing organelle in a
958 marine alga, *Science*, 384, 217-222, 10.1126/science.adk1075, 2024.
- ~~959 Delmont, T. O., Karlusich, J. J. P., Veseli, I., Fuessel, J., Eren, A. M., Foster, R. A., Bowler, C., Wincker, P., and Pelletier, E.:
960 Heterotrophic bacterial diazotrophs are more abundant than their cyanobacterial counterparts in metagenomes covering most
961 of the sunlit ocean, *ISME J*, 16, 927-936, 2022.¶~~
- ~~962 Delmont, T. O., Quince, C., Shaiber, A., Esen, Ö. C., Lee, S. T., Rappé, M. S., MacLellan, S. L., Lückner, S., and Eren, A. M.:
963 Nitrogen-fixing populations of Planctomycetes and Proteobacteria are abundant in surface ocean metagenomes, *Nature*
964 *microbiology*, 3, 804-813, 2018.¶~~
- ~~965 Ding, C., Wu, C., Li, L., Pujari, L., Zhang, G., and Sun, J.: Comparison of Diazotrophic Composition and Distribution in the
966 South China Sea and the Western Pacific Ocean, *Biology (Basel)*, 10, 10.3390/biology10060555, 2021.¶~~
- ~~967 Edgar, R.: UCHIME2: improved chimera prediction for amplicon sequencing, *BioRxiv*, doi.org/10.1101/074252, 2016.¶~~
- ~~968 Falcon Quince, C., Shaiber, A., Esen, Ö. C., Lee, S. T., Rappé, M. S., MacLellan, S. L., Lückner, S., and Eren, A. M.:
969 Nitrogen-fixing populations of Planctomycetes and Proteobacteria are abundant in surface ocean metagenomes, *Nature*
970 *microbiology*, 3, 804-813, 2018.~~
- ~~971 Delmont, T. O., Karlusich, J. J. P., Veseli, I., Fuessel, J., Eren, A. M., Foster, R. A., Bowler, C., Wincker, P., and Pelletier, E.:
972 Heterotrophic bacterial diazotrophs are more abundant than their cyanobacterial counterparts in metagenomes covering most
973 of the sunlit ocean, *ISME J*, 16, 927-936, 2022.~~
- ~~974 Ding, C., Wu, C., Li, L., Pujari, L., Zhang, G., and Sun, J.: Comparison of Diazotrophic Composition and Distribution in the
975 South China Sea and the Western Pacific Ocean, *Biology (Basel)*, 10, 10.3390/biology10060555, 2021.~~
- ~~976 Edgar, R.: UCHIME2: improved chimera prediction for amplicon sequencing, *BioRxiv*, doi.org/10.1101/074252, 2016a.~~
- ~~977 Edgar, R.: UNOISE2: improved error-correction for Illumina 16S and ITS amplicon sequencing, *BioRxiv*,
978 doi.org/10.1101/081257, 2016b.~~
- ~~979 Eren, A. M., Vineis, J. H., Morrison, H. G., and Sogin, M. L.: A filtering method to generate high quality short reads using
980 Illumina paired-end technology, *PLOS ONE*, 8, 6, e66643, 10.1371/journal.pone.0066643, 2013.~~
- ~~981 Eren, A. M., Morrison, H. G., Lescault, P. J., Reveillaud, J., Vineis, J. H. and Sogin, M. L.: Minimum entropy
982 decomposition: Unsupervised oligotyping for sensitive partitioning of high-throughput marker gene sequences, *ISME J*, 9, 4,
983 968-979, doi.org/10.1038/ismej.2014.195, 2014.~~

- 984 Falcón, L., Cipriano, F., Chistoserdov, A., and Carpenter, E.: Diversity of diazotrophic unicellular cyanobacteria in the
985 tropical North Atlantic Ocean, *Appl Environ Microbiol*, 68, 5760, 2002.
- 986 Falcón, L., Carpenter, E., Cipriano, F., Bergman, B., and Capone, D.: N₂ fixation by unicellular bacterioplankton from
987 the Atlantic and Pacific Oceans: phylogeny and in situ rates, *Appl Environ Microbiol*, 70, 765-770, 2004.
- 988 Farnelid, H., Oberg, T., and Riemann, L.: Identity and dynamics of putative N₂-fixing picoplankton in the Baltic Sea proper
989 suggest complex patterns of regulation, *Environmental Microbiology Reports*, 1, 145-154,
990 10.1111/j.1758-2229.2009.00021.x, 2009.
- 991 Farnelid, H., Andersson, A. F., Bertilsson, S., Al-Soud, W. A., Hansen, L. H., Sørensen, S., Steward, G. F., Hagström, A.,
992 and Riemann, L.: Nitrogenase gene amplicons from global marine surface waters are dominated by genes of
993 non-cyanobacteria, *PLOS ONE*, 6, e19223, 10.1371/journal.pone.0019223, 2011.
- 994 Fernandez, C., Farias, L., and Ulloa, O.: Nitrogen fixation in denitrified marine waters, *PLOS ONE*, 6, e20539,
995 10.1371/journal.pone.0020539, 2011.
- 996 Fernandez-Mendez, M., Turk-Kubo, K. A., Buttigieg, P. L., Rapp, J. Z., Krumpfen, T., Zehr, J. P., and Boetius, A.: Diazotroph
997 Diversity in the Sea Ice, Melt Ponds, and Surface Waters of the Eurasian Basin of the Central Arctic Ocean, *Front Microbiol*,
998 7, 1-18, 10.3389/fmicb.2016.01884, 2016.
- 999 Frank, I. E., Turk-Kubo, K. A., and Zehr, J. P.: Rapid annotation of *nifH* gene sequences using classification and regression
1000 trees facilitates environmental functional gene analysis, *Env Microbiol Rep*, 8, 905-916, 2016.
- 1001 Gaby, J. C. and Buckley, D. H.: A global census of nitrogenase diversity, *Environ Microbiol*, 13, 1790-1799,
1002 10.1111/j.1462-2920.2011.02488.x, 2011.
- 1003 Goto, M., Ando, S., Hachisuka, Y., and Yoneyama, T.: Contamination of diverse *nifH* and *nifH*-like DNA into commercial
1004 PCR primers, *FEMS Microbiol Lett*, 246, 33-38, 10.1016/j.femsle.2005.03.042, 2005.
- 1005 Gradoville, M. R., Bombar, D., Crump, B. C., Letelier, R. M., Zehr, J. P., and White, A. E.: Diversity and activity of
1006 nitrogen-fixing communities across ocean basins, *Limnol Oceanogr*, 62, 1895-1909, 2017.
- 1007 Gradoville, M. R., Farnelid, H., White, A. E., Turk-Kubo, K. A., Stewart, B., Ribalet, F., Ferrón, S., Pinedo-Gonzalez, P.,
1008 Armbrust, E. V., Karl, D. M., John, S., and Zehr, J. P.: Latitudinal constraints on the abundance and activity of the
1009 cyanobacterium UCYN-A and other marine diazotrophs in the North Pacific, *Limnol Oceanogr*, 65, 1858-1875,
1010 10.1002/lno.11423, 2020.
- 1011 Green, S. J., Venkatramanan, R., and Naqib, A.: Deconstructing the polymerase chain reaction: Understanding and correcting
1012 bias associated with primer degeneracies and primer-template mismatches, *PLOS ONE*, 10, e0128122,
1013 doi:10.1371/journal.pone.0128122, 2015.
- 1014 Hallstrøm, S., Benavides, M., Salamon, E. R., Arístegui, J., and Riemann, L.: Activity and distribution of diazotrophic
1015 communities across the Cape Verde Frontal Zone in the Northeast Atlantic Ocean, *Biogeochem*, 1-19, 2022a.
- 1016 Hallstrøm, S., Benavides, M., Salamon, E. R., Evans, C. W., Potts, L. J., Granger, J., Tobias, C. R., Moisaner, P. H., and
1017 Riemann, L.: Pelagic N₂ fixation dominated by sediment diazotrophic communities in a shallow temperate estuary, *Limnol*
1018 *Oceanogr*, 67, 364-378, 2022b.

- 1019 Halm, H., Lam, P., Ferdelman, T. G., Lavik, G., Dittmar, T., LaRoche, J., D'Hondt, S., and Kuypers, M. M.: Heterotrophic
1020 organisms dominate nitrogen fixation in the South Pacific Gyre, *ISME J*, 6, 1238-1249, 10.1038/ismej.2011.182, 2012.
- 1021 Harding, K., Turk-Kubo, K. A., Sipler, R. E., Mills, M. M., Bronk, D. A., and Zehr, J. P.: Symbiotic unicellular
1022 cyanobacteria fix nitrogen in the Arctic Ocean, *Proc Natl Acad Sci U S A*, 115, 13371-13375, 10.1073/pnas.1813658115,
1023 2018.
- 1024 Heller, P., Tripp, H. J., Turk-Kubo, K., and Zehr, J. P.: ARBitrator: a software pipeline for on-demand retrieval of
1025 auto-curated *nifH* sequences from GenBank, *Bioinformatics*, 10.1093/bioinformatics/btu417, 2014.
- 1026 Jickells, T., Buitenhuis, E., Altieri, K., Baker, A., Capone, D., Duce, R., Dentener, F., Fennel, K., Kanakidou, M., and
1027 LaRoche, J.: A reevaluation of the magnitude and impacts of anthropogenic atmospheric nitrogen inputs on the ocean,
1028 *Global Biogeochem. Cy.*, 31, 289-305, 2017.
- 1029 Langlois, R. J., LaRoche, J., and Raab, P. A.: Diazotrophic diversity and distribution in the tropical and subtropical Atlantic
1030 Ocean, *Appl Environ Microbiol*, 71, 7910-7919, 10.1128/AEM.71.12.7910-7919.2005, 2005.
- 1031 Langlois, R., Großkopf, T., Mills, M., Takeda, S., and LaRoche, J.: Widespread distribution and expression of Gamma A
1032 (UMB), an uncultured, diazotrophic, γ -proteobacterial *nifH* phylotype, *PLOS ONE*, 10, e0128912, 2015.
- 1033 ~~Langlois, R. J., LaRoche, J., and Raab, P. A.: Diazotrophic diversity and distribution in the tropical and subtropical Atlantic
1034 Ocean, *Appl Environ Microbiol*, 71, 7910-7919, 10.1128/AEM.71.12.7910-7919.2005, 2005.~~
- 1035 Liu, J., Zhou, L., Li, J., Lin, Y., Ke, Z., Zhao, C., Liu, H., Jiang, X., He, Y., and Tan, Y.: Effect of mesoscale eddies on
1036 diazotroph community structure and nitrogen fixation rates in the South China Sea, *Regional Studies in Marine Science*, 35,
1037 101106, 2020.
- 1038 Löscher, C. R., Großkopf, T., Desai, F. D., Gill, D., Schunck, H., Croot, P. L., Schlosser, C., Neulinger, S. C., Pinnow, N.,
1039 and Lavik, G.: Facets of diazotrophy in the oxygen minimum zone waters off Peru, *ISME J*, 8, 2180-2192, 2014.
- 1040 Luo, Y. W., Doney, S. C., Anderson, L. A., Benavides, M., Berman-Frank, I., Bode, A., Bonnet, S., Boström, K. H., Böttjer,
1041 D., Capone, D. G., Carpenter, E. J., Chen, Y. L., Church, M. J., Dore, J. E., Falcón, L. I., Fernández, A., Foster, R. A.,
1042 Furuya, K., Gómez, F., Gundersen, K., Hynes, A. M., Karl, D. M., Kitajima, S., Langlois, R. J., LaRoche, J., Letelier, R. M.,
1043 Marañón, E., McGillicuddy, D. J., Moisaner, P. H., Moore, C. M., Mouriño-Carballido, B., Mulholland, M. R., Needoba, J.
1044 A., Orcutt, K. M., Poulton, A. J., Rahav, E., Raimbault, P., Rees, A. P., Riemann, L., Shiozaki, T., Subramaniam, A., Tyrrell,
1045 T., Turk-Kubo, K. A., Varela, M., Villareal, T. A., Webb, E. A., White, A. E., Wu, J., and Zehr, J. P.: Database of diazotrophs
1046 in global ocean: abundance, biomass and nitrogen fixation rates, *Earth System Science Data*, 4, 47-73,
1047 10.5194/essd-4-47-2012, 2012.
- 1048 Manley, L. J., Ma, D., and Levine, S. S.: Monitoring error rates In *Illumina sequencing*, *J Biomol Tech*, 27, 4, 125-128,
1049 10.7171/jbt.16-2704-002, 2016.
- 1050 Martin, M.: Cutadapt removes adapter sequences from high-throughput sequencing reads, *EMBnet*, 17, 10-12, 2011.
- 1051 Messer, L. F., Mahaffey, C., Robinson, C. M., Jeffries, T. C., Baker, K. G., Isaksson, J. B., Ostrowski, M., Doblin, M. A.,
1052 Brown, M. V., and Seymour, J. R.: High levels of heterogeneity in diazotroph diversity and activity within a putative hotspot
1053 for marine nitrogen fixation, *ISME J*, 1499-1513, 2015.
- 1054 Moisaner, P. H., Beinart, R. A., Voss, M., and Zehr, J. P.: Diversity and abundance of diazotrophic microorganisms in the
1055 South China Sea during intermonsoon, *ISME J*, 2, 954-967, 10.1038/ismej.2008.51, 2008.

- 1056 Moisander, P. H., Serros, T., Paerl, R. W., Beinart, R. A., and Zehr, J. P.: Gammaproteobacterial diazotrophs and *nifH* gene
1057 expression in surface waters of the South Pacific Ocean, *ISME J*, 8, 1962-1973, 10.1038/ismej.2014.49, 2014.
- 1058 Moisander, P. H., Benavides, M., Bonnet, S., Berman-Frank, I., White, A. E., and Riemann, L.: Chasing after
1059 non-cyanobacterial nitrogen fixation in marine pelagic environments, *Front Microbiol*, 8, 1736, 2017.
- 1060 Moonsamy, P. V., Williams, T., Bonella, P., Holcomb, C. L., Hoglund, B. N., Hillman, G., Goodridge, D., Turenchalk, G. S.,
1061 Blake, L. A., Daigle, D. A., Simen, B. B., Hamilton, A., May, A. P., and Erlich, H. A.: High throughput HLA genotyping
1062 using 454 sequencing and the Fluidigm Access Array System for simplified amplicon library preparation, *Tissue Antigens*,
1063 81, 141-149, 10.1111/tan.12071, 2013.
- 1064 Morando, M., Magasin, J., Cheung, S., Mills, M. M., Zehr, J. P., and Turk-Kubo, K. A.: *nifH* ASV database in Global
1065 biogeography of N₂-fixing microbes: *nifH* amplicon database and analytics workflow, *Figshare* [dataset],
1066 <https://doi.org/10.6084/m9.figshare.23795943.v1>, 2024v2, 2024a.
- 1067 Morando, M., Magasin, J., Cheung, S., Mills, M. M., Zehr, J. P., and Turk-Kubo, K. A.: DADA2 *nifH* pipeline in Global
1068 biogeography of N₂-fixing microbes: *nifH* amplicon database and analytics workflow, *GitHub* [code],
1069 https://github.com/jdmagasin/nifH_amplicons_DADA2, 2024b.
- 1070 Morando, M., Magasin, J., Cheung, S., Mills, M. M., Zehr, J. P., and Turk-Kubo, K. A.: *nifH* ASV workflow in Global
1071 biogeography of N₂-fixing microbes: *nifH* amplicon database and analytics workflow, *GitHub* [code],
1072 <https://github.com/jdmagasin/nifH-ASV-workflow>, 2024c.
- 1073 Mulholland, M. R., Bernhardt, P. W., Widner, B. N., Selden, C. R., Chappell, P. D., Clayton, S., Mannino, A., and Hyde, K.:
1074 High Rates of N₂ Fixation in Temperate, Western North Atlantic Coastal Waters Expand the Realm of Marine Diazotrophy,
1075 *Global Biogeochem. Cy.*, 33, 826-840, 10.1029/2018gb006130, 2019.
- 1076 Pierella Karlusich, J. J., Pelletier, E., Lombard, F., Carsique, M., Dvorak, E., Colin, S., Picheral, M., Cornejo-Castillo, F. M.,
1077 Acinas, S. G., Pepperkok, R., Karsenti, E., de Vargas, C., Wincker, P., Bowler, C., and Foster, R. A.: Global distribution
1078 patterns of marine nitrogen-fixers by imaging and molecular methods, *Nat Commun*, 12, 1-18, 10.1038/s41467-021-24299-y,
1079 2021.
- 1080 Quince, C., Lanzén, A., Curtis, T. P., Davenport, R. J., Hall, N., Head, I. M., Read, L. F., and Sloan, W. T.: Accurate
1081 determination of microbial diversity from 454 pyrosequencing data, *Nat Methods*, 6, 639-641, doi.org/10.1038/nmeth.1361,
1082 2009.
- 1083 Raes, E. J., Van de Kamp, J., Bodrossy, L., Fong, A. A., Riekenberg, J., Holmes, B. H., Erler, D. V., Eyre, B. D., Weil, S. S.,
1084 and Waite, A. M.: N₂ fixation and new insights into nitrification from the ice-edge to the equator in the South Pacific Ocean,
1085 *Frontiers in Marine Science*, 7, 1-20, 2020.
- 1086 Rho, M., Tang, H., and Ye, Y.: FragGeneScan: predicting genes in short and error-prone reads, *Nucleic Acids Res*, 38, e191,
1087 10.1093/nar/gkq747, 2010.
- 1088 Rognes, T., Flouri, T., Nichols, B., Quince, C., and Mahe, F.: VSEARCH: a versatile open source tool for metagenomics,
1089 *PeerJ*, 4, e2584, 10.7717/peerj.2584, 2016.
- 1090 Sato, T., Shiozaki, T., Taniuchi, Y., Kasai, H., and Takahashi, K.: Nitrogen Fixation and Diazotroph Community in the
1091 Subarctic Sea of Japan and Sea of Okhotsk, *Journal of Geophysical Research: Oceans*, 126, e2020JC017071, 2021.

- 1092 Schlessman, J. L., Woo, D., Joshua-Tor, L., Howard, J. B., and Rees, D. C.: Conformational variability in structures of the
1093 nitrogenase iron proteins from *Azotobacter vinelandii* and *Clostridium pasteurianum*, *J Mol Biol*, 280, 4, 669-685, 1998.
- 1094 Selden, C. R., Chappell, P. D., Clayton, S., Macías-Tapia, A., Bernhardt, P. W., and Mulholland, M. R.: A coastal N₂ fixation
1095 hotspot at the Cape Hatteras front: Elucidating spatial heterogeneity in diazotroph activity via supervised machine learning,
1096 *Limnol Oceanogr*, 66, 1832-1849, 2021.
- 1097 Shao, Z. and Luo, Y. W.: Controlling factors on the global distribution of a representative marine heterotrophic diazotroph
1098 phylotype (Gamma A), *Biogeosciences*, 19, 2939-2952, 2022.
- 1099 Shao, Z., Xu, Y., Wang, H., Luo, W., Wang, L., Huang, Y., Agawin, N. S. R., Ahmed, A., Benavides, M., Bentzon-Tilia, M.,
1100 and Berman-Frank, I.: Global Oceanic Diazotroph Database Version 2 and Elevated Estimate of Global N₂ Fixation, *Earth*
1101 *System Science Data*, 15, 2023.
- 1102 Shilova, I., Mills, M., Robidart, J., Turk-Kubo, K., Björkman, K., Kolber, Z., Rapp, I., van Dijken, G., Church, M., and
1103 Arrigo, K.: Differential effects of nitrate, ammonium, and urea as N sources for microbial communities in the North Pacific
1104 Ocean, *Limnol Oceanogr*, 62, 2550-2574, 2017.
- 1105 Shiozaki, T., Fujiwara, A., Inomura, K., Hirose, Y., Hashihama, F., and Harada, N.: Biological nitrogen fixation detected
1106 under Antarctic sea ice, *Nature Geoscience*, 13, 729–732, 2020.
- 1107 Shiozaki, T., Fujiwara, A., Ijichi, M., Harada, N., Nishino, S., Nishi, S., Nagata, T., Bombar, D., Riemann, L., Hashihama, F.,
1108 Takeda, S., Yamaguchi, T., Ehama, M., Hamasaki, K., and Hamasaki-Furuya, K.: Diazotroph community structure and the
1109 role of nitrogen fixation in the nitrogen cycle in the Chukchi Sea (western Arctic Ocean), *Limnol Oceanogr*, 63, 2191-2205,
1110 [10.1002/lno.10933](https://doi.org/10.1002/lno.10933), 2018a.
- 1111 Shiozaki, T., Bombar, D., Riemann, L., Hashihama, F., Takeda, S., Yamaguchi, T., Ehama, M., Hamasaki, K. Basin scale
1112 variability of active diazotrophs and nitrogen fixation in the North Pacific, from the tropics to the subarctic Bering Sea,
1113 *Global Biogeochem. Cy.*, 31, 996-1009, [10.1002/2017gb005681](https://doi.org/10.1002/2017gb005681), 2017.
- 1114 Shiozaki, T., Fujiwara, A., Ijichi, M., Harada, N., Nishino, S., Nishi, S., Nagata, T., and Furuya-Hamasaki, K.: Basin scale
1115 variability of active diazotrophs and nitrogen fixation in the North Pacific, from the tropics to the subarctic Bering Sea,
1116 *Global Biogeochem. Cy.*, 31, 996-1009, [10.1002/2017gb005681](https://doi.org/10.1002/2017gb005681), 2017. Diazotroph community structure and the role of
1117 nitrogen fixation in the nitrogen cycle in the Chukchi Sea (western Arctic Ocean), *Limnol Oceanogr*, 63, 2191-2205,
1118 [10.1002/lno.10933](https://doi.org/10.1002/lno.10933), 2018a.
- 1119 Shiozaki, T., Bombar, D., Riemann, L., Sato, M., Hashihama, F., Kodama, T., Tanita, I., Takeda, S., Saito, H., Hamasaki, K.,
1120 and Furuya, K.: Linkage between dinitrogen fixation and primary production in the oligotrophic South Pacific Ocean, *Global*
1121 *Biogeochem. Cy.*, 32, 1028-1044, 2018b.
- 1122 Tang, W., Li, Z., and Cassar, N.: Machine learning estimates of global marine nitrogen fixation, *Journal of Geophysical*
1123 *Research: Biogeosciences*, 124, 717-730, 2019.
- 1124 Tang, W., Cerdan-Garcia, E., Berthelot, H., Polyviou, D., Wang, S., Baylay, A., Whitby, H., Planquette, H., Mowlem, M.,
1125 Robidart, J., and Cassar, N.: New insights into the distributions of nitrogen fixation and diazotrophs revealed by
1126 high-resolution sensing and sampling methods, *ISME J*, 14, 2514-2526, [10.1038/s41396-020-0703-6](https://doi.org/10.1038/s41396-020-0703-6), 2020.
- 1127 Taylor, L. J., Abbas, A., and Bushman, F. D.: grabseqs: Simple downloading of reads and metadata from multiple
1128 next-generation sequencing data repositories, *Bioinformatics*, doi.org/10.1093/bioinformatics/btaa167, 2020.

- 1129 Turk, K., Rees, A. P., Zehr, J. P., Pereira, N., Swift, P., Shelley, R., Lohan, M., Woodward, E. M. S., and Gilbert, J.: Nitrogen
 1130 fixation and nitrogenase (*nifH*) expression in tropical waters of the eastern North Atlantic, ISME J, 5, 1201-1212,
 1131 10.1038/ismej.2010.205, 2011.
- 1132 Turk-Kubo, K. A., Karamchandani, M., Capone, D. G., and Zehr, J. P.: The paradox of marine heterotrophic nitrogen
 1133 fixation: abundances of heterotrophic diazotrophs do not account for nitrogen fixation rates in the Eastern Tropical South
 1134 Pacific, Environ Microbiol, 16, 3095-3114, 10.1111/1462-2920.12346, 2014.
- 1135 Turk-Kubo, K. A., Farnelid, H. M., Shilova, I. N., Henke, B., and Zehr, J. P.: Distinct ecological niches of marine symbiotic
 1136 N₂-fixing cyanobacterium *Candidatus Atelocyanobacterium thalassa* sublineages, J Phycol, 53, 451-461, 10.1111/jpy.12505,
 1137 2017.
- 1138 Turk-Kubo, K. A., ~~Gradoville~~Mills, M. R., Cheung, S., Cornejo-Castillo, F., Harding, K. J., Morando, M., Mills, M., and
 1139 Zehr, J. P.: ~~Non-cyanobacterial diazotrophs: Global diversity, distribution, ecophysiology, and activity in marine waters,~~
 1140 ~~FEMS Microbiol Rev, 10.1093/femsre/fuac046, 2022~~M., Arrigo, K. R., van Dijken, G., Henke, B. A., Stewart, B., Wilson, S.
 1141 T., and Zehr, J. P.: UCYN-A/haptophyte symbioses dominate N₂ fixation in the Southern California Current System, ISME
 1142 Communications, 1, 1-13, 2021.
- 1143 Turk-Kubo, K. A., ~~Mills~~Gradoville, M. M., Arrigo, K. R., van Dijken, G., Henke, B. A., Stewart, B., Wilson, S. T., and Zehr,
 1144 J. P.: ~~UCYN A/haptophyte symbioses dominate N₂ fixation in the Southern California Current System, ISME~~
 1145 ~~Communications, 1, 1-13, 2021~~R., Cheung, S., Cornejo-Castillo, F., Harding, K. J., Morando, M., Mills, M., and Zehr, J. P.:
 1146 ~~Non-cyanobacterial diazotrophs: Global diversity, distribution, ecophysiology, and activity in marine waters, FEMS~~
 1147 ~~Microbiol Rev, 10.1093/femsre/fuac046, 2022.~~
- 1148 Villareal, T. A.: Widespread occurrence of the *Hemiaulus*-cyanobacterial symbiosis in the southwest North-Atlantic Ocean,
 1149 Bulletin of Marine Science, 54, 1-7, 1994.
- 1150 Wu, C., Kan, J., Liu, H., Pujari, L., Guo, C., Wang, X., and Sun, J.: Heterotrophic Bacteria Dominate the Diazotrophic
 1151 Community in the Eastern Indian Ocean (EIO) during Pre-Southwest Monsoon, Microb Ecol, 78, 804-819,
 1152 10.1007/s00248-019-01355-1, 2019.
- 1153 Wu, C., Sun, J., Liu, H., Xu, W., Zhang, G., Lu, H., and Guo, Y.: Evidence of the Significant Contribution of Heterotrophic
 1154 Diazotrophs to Nitrogen Fixation in the Eastern Indian Ocean During Pre-Southwest Monsoon Period, Ecosyst, 25,
 1155 1066-1083, 2021.
- 1156 Zani, S.: Application of a nested reverse transcriptase polymerase chain reaction assay for the detection of *nifH* expression in
 1157 Lake George, New York, M. S. Thesis, Rensselaer Polytechnic Institute, 1999.
- 1158 Zehr, J. P. and Capone, D. G.: Changing perspectives in marine nitrogen fixation, Science, 368, eaay9514,
 1159 10.1126/science.aay9514, 2020.
- 1160 Zehr, J. and McReynolds, L.: Use of degenerate oligonucleotides for amplification of the *nifH* gene from the marine
 1161 cyanobacterium *Trichodesmium thiebautii*, Appl Environ Microbiol, 55, 2522-2526, 1989.
- 1162 Zehr, J., Mellon, M., and Zani, S.: New nitrogen-fixing microorganisms detected in oligotrophic oceans by amplification of
 1163 nitrogenase (*nifH*) genes, Appl. Environ. Microbiol, 64, 3444-3450, 1998.
- 1164 Zehr, J. P. and Capone, D. G.: ~~Changing perspectives in marine nitrogen fixation, Science, 368, eaay9514,~~
 1165 ~~10.1126/science.aay9514, 2020.~~

- ~~1166 Zehr, J. P., Crumbliss, L. L., Church, M. J., Omoregie, E. O., and Jenkins, B. D.: Nitrogenase genes in PCR and RT-PCR
1167 reagents: implications for studies of diversity of functional genes, Biotechniques, 35, 996-1005, 2003.¶~~
- 1168 Zehr, J. P., Waterbury, J. B., Turner, P. J., Montoya, J. P., Omoregie, E., Steward, G. F., Hansen, A., and Karl, D. M.:
1169 Unicellular cyanobacteria fix N₂ in the subtropical North Pacific Ocean, Nature, 412, 635-638, 2001.
1170
- 1171 Zehr, J. P., Crumbliss, L. L., Church, M. J., Omoregie, E. O., and Jenkins, B. D.: Nitrogenase genes in PCR and RT-PCR
1172 reagents: implications for studies of diversity of functional genes, Biotechniques, 35, 996-1005, 2003.